Supercritical CO2 Power Technology: Strengths but Challenges

Michel Molière, Romain Privat, Jean-Noël Jaubert, Frédéric Geiger

energies

Article

Supercritical CO_2 Power Technology: Strengths but Challenges

Michel Molière [1,2,*], Romain Privat [1], Jean-Noël Jaubert [1] and Frédéric Geiger [3]

[1] Laboratoire Réactions et Génie des Procédés, Université de Lorraine, 54000 Nancy, France; romain.privat@univ-lorraine.fr (R.P.); jean-noel.jaubert@univ-lorraine.fr (J.-N.J.)
[2] Institut Carnot de Bourgogne-Université de Technologie de Belfort Montbéliard (ICB-UTBM), 90000 Belfort, France
[3] Département Sciences et Énergies, UFR-STGI, Université de Franche-Comté, 90000 Belfort, France; fgeiger2@wanadoo.fr
* Correspondence: michel.moliere@utbm.fr

Abstract: In the late 1960s, a handful of inspired researchers predicted the great potential of supercritical CO_2 ("sCO_2") cycles for the production of electricity and highlighted the prospects for dramatic reductions in component sizes and efficiency increases. Since then, considerable development programs have been deployed around the world to "tame" this new technology. Despite these efforts, in-depth engineering studies and extensive testing are still necessary today before viable designs can be released for large-scale industrial applications. This raises questions as to the reasons for this delay, this debate being rarely addressed in the current literature. This situation has motivated the present study. Trying to unravel such an intricate topic requires to understand the distinctive properties of supercritical CO_2 and the particular requirements of closed, high-pressure power systems. This article aims then to provide a broad overview of sCO_2 power cycles, highlighting their main advantages and limitations and reflecting the challenges associated with the industrialization of that technology which actually requires disruptive and innovative designs.

Keywords: supercritical CO_2; electric power; thermodynamic cycle; Rankine; Brayton

Citation: Molière, M.; Privat, R.; Jaubert, J.-N.; Geiger, F. Supercritical CO_2 Power Technology: Strengths but Challenges. *Energies* **2024**, *17*, 1129. https://doi.org/10.3390/en17051129

Academic Editor: Adam Smoliński

Received: 23 January 2024
Revised: 12 February 2024
Accepted: 23 February 2024
Published: 27 February 2024

1. Introduction

The use of sCO_2 cycles to produce electric power is an emerging technology which is expected to bring substantial efficiency gains. This power generation route then attracts the interest of the power community, including producers and major OEMs as it would also reduce the size of cycle components and thus decrease the CAPEX of power plants.

However, during successive development attempts, initially carried out on small test loops, the experimenters faced technical issues which prevented the rapid release of viable pilot units. These difficulties, not anticipated by the precursors of the technology, are linked to marked specificities of sCO_2 cycles, in particular their high pressures but low-pressure ratios, the difficulty of controlling CO_2 leaks and the unusually small dimensions of certain components, which require unconventional designs. That technology is therefore still in the engineering and testing phase, with the most consistent and active program being currently the so-called "Supercritical Transformational Electric Power" (STEP), funded by the US Department of Energy (DOE) [1,2].

While questions legitimately arise about the reasons for this industrialization delay, this discussion is still little reflected in the academic literature.

The primary objective of this study was to tentatively fill this gap by investigating the main technical specificities and potential design obstacles which cause this long industrialization process. However, attempting to clarify such a complex and far-reaching topic required an in-depth approach to sCO_2 cycles in order to understand how the specificities of these cycles impact the engineering of large power systems.

This led us to adopt the following paper plan: after a brief history and some basic definitions (Sections 2 and 3), we will identify the specificities of sCO_2 cycles and deduce

the associated advantages and drawbacks (Section 4). We will then review their possible architectures in Section 5. In Section 6, we will evaluate their performance in two paradigmatic applications (solar and heat recovery) and compare them to those of conventional steam Rankine cycles: this will tell us whether these cycles can compete with existing power systems. Finally, in Sections 7 and 8, we will review the status of technical developments made to date and try to identify the technological barriers to overcome to design large prototype units, with power outputs greater than, say, 20 MWe.

In this approach, we will cover both Rankine and Brayton closed cycles but not the semi-closed ones, i.e., the Allam cycles which feature very specific designs [3].

2. Brief History

In the late 1960s, a small number of scientists (Angelino in Italy [4–6]; Feher in the USA [7,8]; Gokhstein and Verhivker in the former USSR [9]) laid the foundations for the sCO_2 technology as a path to efficient power generation.

After three decades during which these pioneering works were neglected [10], a series of development programs began mainly in the USA, Japan and Korea, using test rigs of a few dozen kWe [11–18]. However, these tests revealed a series of unexpected and arduous issues, including disturbing CO_2 leaks that proved difficult to control; operation instabilities with difficulties reaching stationary loads and thermal stresses experienced by turbine materials at temperatures above 500 °C. Therefore, although significant progress has been made in understanding the general requirements of this technology in terms of hardware, systems and controls, these programs have not to date resulted in a generic prototype designs suitable for large power blocks.

Nevertheless, the so-called SunShot project launched in 2011 by the US DOE and teamed by SwRI and GE has delivered fruitful design concepts for small-size units, namely for a 1 MW, 715 °C turbine able to rotate at 27,000 rpm [19,20]. Incidentally, it should be noted that the designs created for small turbomachines running at such high speeds cannot be directly extrapolated, for mechanical reasons, to large turbogenerators which must instead rotate at 3600 or 3000 rpm.

More recently (2016), the DOE launched the STEP project intended to deliver industrial sCO_2 power units of the 10 MWe size [21,22]. This program is based on a 16 MW turbine prototype and is led by the GTI, SwRI and GE forming the main partners of a dedicated Joint Industrial Program (JIP). It is important to mention that the STEP pilot plant is actually equipped with quite large thermal components, namely a 93 MWth CO_2 heater and a 50 MWth heat recuperator, which will allow further scale-ups of future prototypes [23].

Since sCO_2 power cycles are the subject of numerous academic articles which do not, however, address the theme of industrialization, reference [24] can be consulted for a broad and recent review of these publications.

In this paper, the term "sCO_2" will refer to any thermodynamic cycle that involves supercritical CO_2 in at least one of its stages.

The notations P– and P+ (respectively T– and T+) will designate the low and high pressure (respectively temperature) levels of the cycles. Thermodynamic simulations were carried with SimulisThermodynamics® and Prosimplus® software.

3. How to Define sCO_2 Cycles in Relation to Conventional Ones?

Most large power units are based on turbomachines and operate essentially according to steam Rankine(-Hirn) or air Brayton cycles or combinations of both. Figure 1 provides a simplified classification of the main types of such large power cycles based on H_2O, air and CO_2, according to their sub-, trans- and supercritical character:

- Diagram A shows two subcritical cycles: [A … → D] (steam Rankine) and [1 … → 4] (air Brayton)
- Diagram B sketches a "true" supercritical CO_2 Brayton cycle: all stages are performed at P > Pc and T > Tc; in other terms, all are located in the supercritical region and there is no condensation step

- Diagram C represents two "wet transcritical" cycles that use H_2O ([a… → d]) and CO_2 ([A… → D]) as respective fluids; stages A → B (and a → b) are performed in the supercritical region; condensation occurs at stages E → A and d → a, respectively; these are Rankine cycles in their simplest form
- Diagram D refers to a "dry transcritical" CO_2 cycle: in this variant, we bypass the condensation step using a sequence of compression and cooling stages, whose details will be given in paragraph 4.2.3; this cycle can be assimilated to an intercooled Brayton.

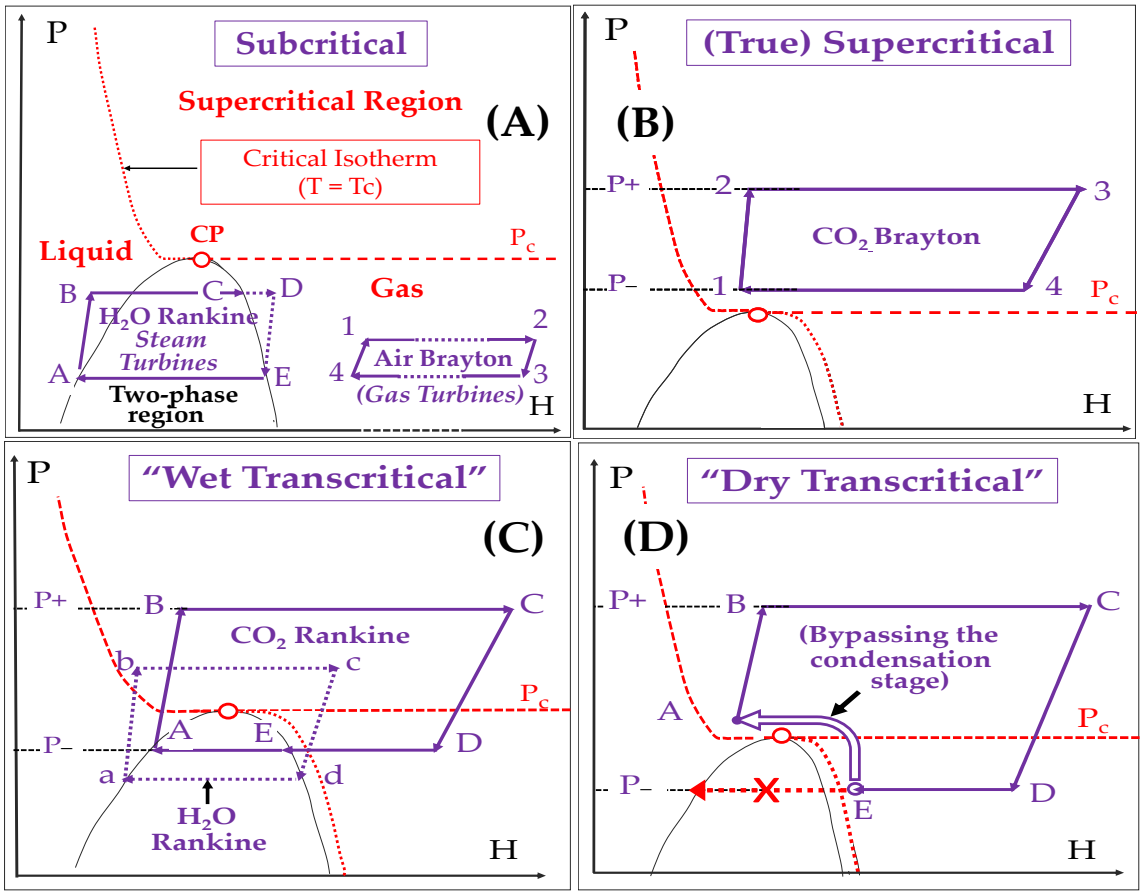

Figure 1. Main basic types of large power cycles using CO_2, air or H_2O as fluids: (**A**): Subcritical; (**B**): (True) Supercritical; (**C**): Wet Transcritical; (**D**): Dry Transcritical.

It should be stressed that actual industrial cycles are much more sophisticated.

4. Fundamental Properties of sCO_2 Cycles

In this section, we will focus on the "conceptual" advantages and drawbacks of the sCO_2 technology, which result from the specificities of supercritical fluids [25] and the design of the corresponding cycles.

To do that, we will assume "ideal" conditions, i.e., we will take all isentropic efficiencies of compression and expansion equal to 1 and neglect all pressure drops and mechanical/electrical/magnetic losses. This will of course result in optimistic performances but will provide a common basis on which (i) to quantify the conceptual assets of sCO_2 cycles with respect to conventional ones and (ii) to compare the merits of distinct cycle types and architectures.

Figure 2 shows a general P-H diagram that will be used in our analysis of sCO_2 power cycles. One distinguishes four regions around the critical point ("CP"): the liquid, the supercritical (P > Pc and T > Tc), the real gas and perfect gas regions.

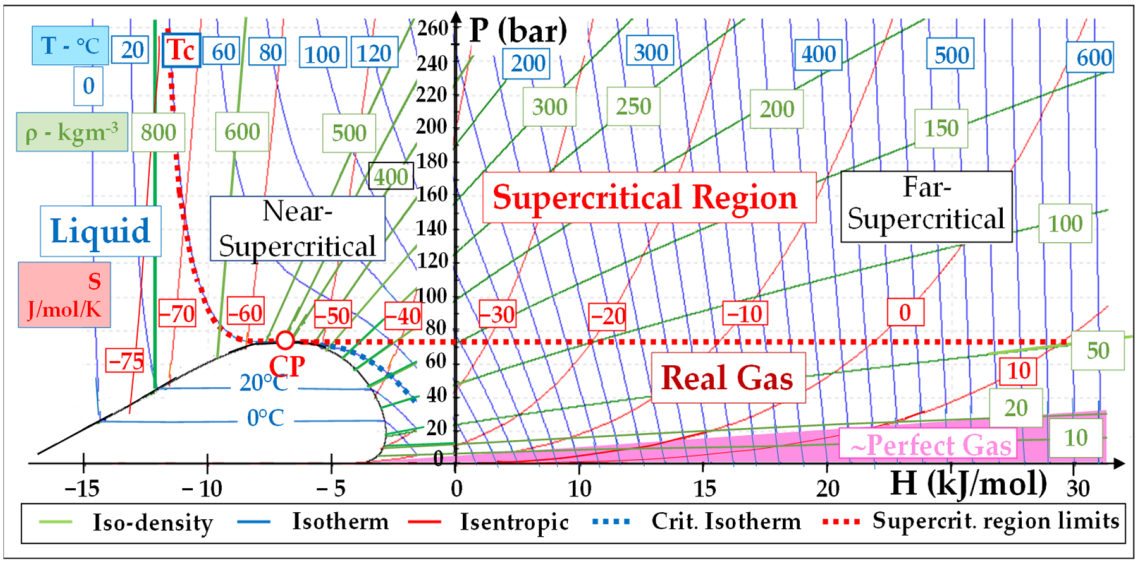

Figure 2. P-H diagram of CO_2 with the temperature, density and entropy isopleths suitable for the representation of sCO_2 power cycles.

The portion of the supercritical region in the lower (respectively high) enthalpy zone will be called "near-supercritical" (respectively "far-supercritical").

4.1. The Conceptual Strengths

The two fundamental advantages of sCO_2 cycles are (1) elevated efficiency and (2) reduced component sizes [26–28]. We will show that both result from a single property, namely the high density of supercritical fluids, as compared to gases and vapors used in the subcritical cycles that are represented in Figure 1A.

4.1.1. Efficient Compression and Expansion Result in High Cycle Efficiency

The elemental compression or expansion work (δw) involving a unit mass of fluid and performed in reversible conditions (i.e., at constant entropy), is given by the following equation:

$$\delta w = dh_S = v.dP = dP/\rho \quad (1)$$

where h and v are the specific enthalpy and volume of the fluid and ρ its density.

In other terms, when the density increases, the corresponding work decreases and vice versa.

When looking now at the iso-density lines plotted in the P-H diagram of Figure 2, we see that:

- Density is high ($\rho \approx 400$–600 kg/m^3) in the zone close to the critical point ("CP"): the "near-supercritical" region
- It decreases (down to 100 kg/m^3) in the higher enthalpy ("far-supercritical") region.
- It still decreases in the "real gas" region ($\rho \approx 50$ kg/m^3) and even more in the nearly-perfect CO_2 (pink area) region: there, ρ drops to around 10 kg/m^3 below 10 bar and its value at 0 °C-1 atm falls to 2 kg/m^3.

Let us look now at a basic (non-recuperated) supercritical cycle (Figure 3) for which we take the following input data: (T–, P–) = (45 °C, 75 bar) and (T+, P+) = (550 °C, 225 bar). From Equation (1), we deduce the following:

- The reversible mechanical work (W_{compr}) consumed for the compression performed in the near-supercritical region is very low; indeed, in stage 1 → 2, ρ = 600 kg/m^3 (Figure 1) and $W_{compr} \approx 3$ kJ/mol.

- Reversely, the expansion work (W_{exp}) which is performed in the far-supercritical region is high; in stage 3 → 4, W_{exp} is approximately equal to 17 kJ/mol.

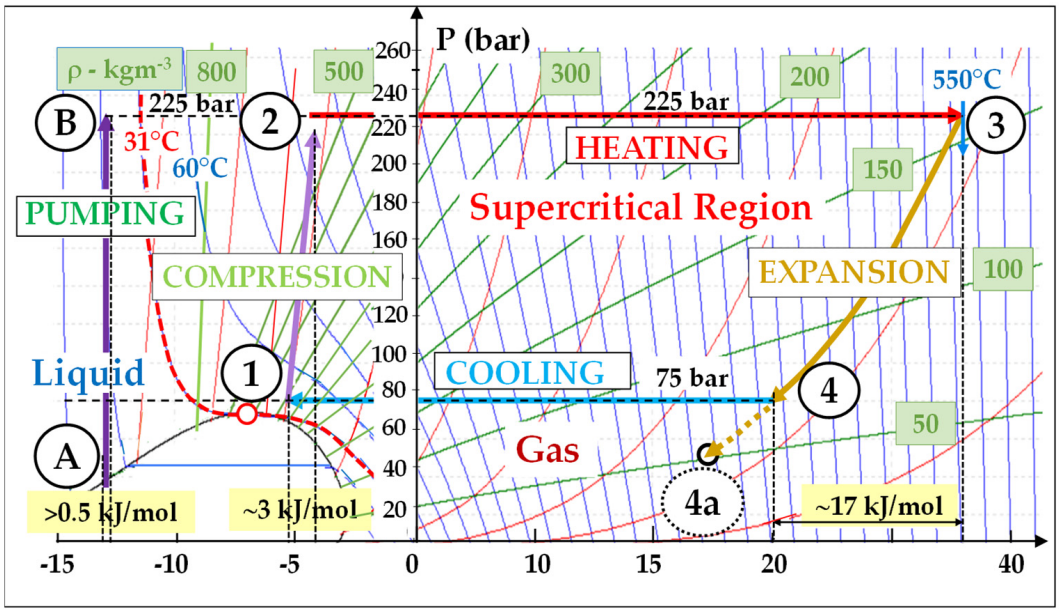

Figure 3. Basic sCO_2 Brayton cycle (non-recuperated: (T–, P–) = (45 °C, 75 bar) − (T+, P+) = (550 °C, 225 bar): W_{compr}/W_{exp} = 3/17 = 0.18; reversible conditions.

Figure 3 shows that the energy consumed by the reversible compression represents approximately 18% of that delivered by the expansion. In comparison, this percentage is about 42% (11/26) in a typical F-class gas turbine, as shown by Figure 4. Moreover, this ratio is still lower in a supercritical steam cycle: around 4%.

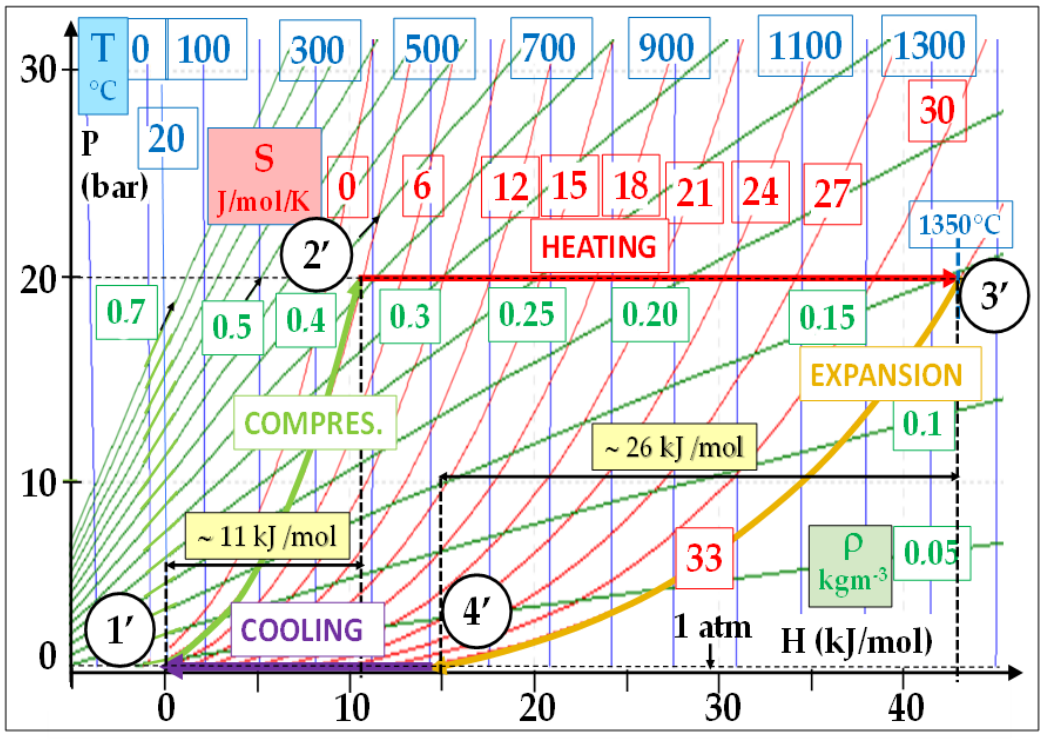

Figure 4. Typical air Brayton cycle: (T–, P–) = (20 °C, 1 atm) − (T+, P+) = (1350 °C, 250 bar); reversible conditions: W_{compr}/W_{exp} = 11/26 = 0.42.

Indeed, we must note that the density is the highest (and W_{compr} the lowest) in the liquid region, where ρ_{CO_2} typically exceeds 800 kg/m^3. This allows for very efficient pumping stages, which represents an inherent efficiency merit of Rankine cycles: for example, the pumping stage A → B ($\rho \approx 900$ kg/m^3) consumes hardly 0.5 kJ/mol (Figure 3).

Such favorable compression and expansion stages result in excellent cycle efficiencies. This will be illustrated by the remarkable performance of the most advanced sCO_2 cycles which will be described in Section 5.

4.1.2. Compactness of sCO_2 Power Units

The second key advantage of sCO_2 cycles is the dramatic reduction in size of cycle components, which is again correlated to the high density of supercritical CO_2 [29,30].

Indeed, to control the level of turbulence of the fluid and minimize the resulting losses in static pressure and efficiency, the cross-section of a turbomachine is designed proportional to the volumetric flow of the fluid, i.e., inversely proportional to its density.

Although the sCO_2 machines have higher mass flow rates (for the reasons that will be set out in paragraph 4.2.1), their sizes are significantly smaller due to the fluid density effect.

Figure 5 presents a notional comparison between the diameters of a sCO_2 turbine and a steam turbine ("ST") that deliver power output of the same order [31]. A quantitative comparison will be proposed below (§ 5.1).

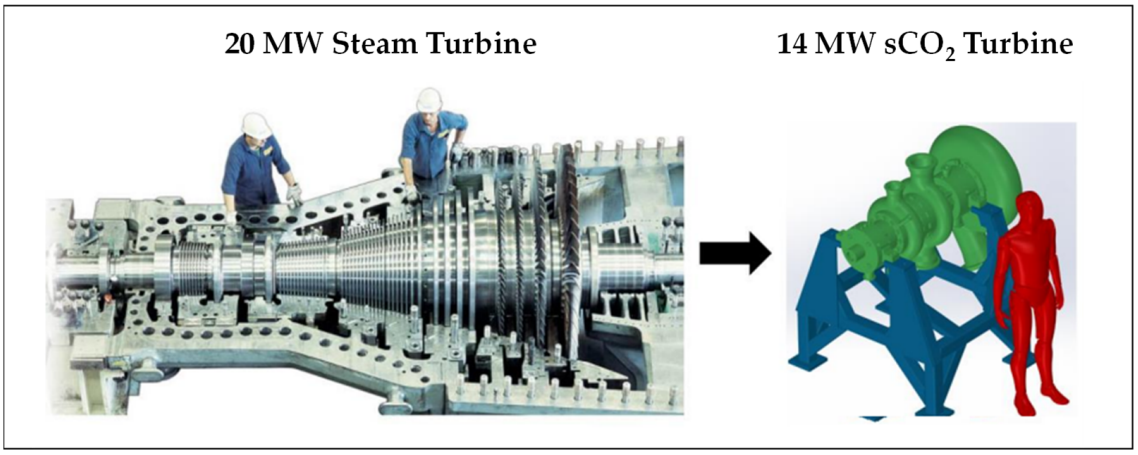

Figure 5. Qualitative comparison between the size of a steam turbine and an sCO_2 turbine [31].

It is worth noting that the rotation speed of the shaft also conditions the size: the higher the speed, the smaller the diameter.

4.1.3. Other Strengths Linked to Favorable Properties of the CO_2 Molecule

SCO_2 cycles have other important merits linked to advantageous properties of the CO_2 molecule.

Firstly, unlike H_2O that has elevated critical properties (374 °C, 221 bar), the critical point of CO_2 is easily accessible (31.1 °C, 73.8 bars).

Additionally, compared to hydrocarbons used in Organic Rankine Cycles (ORC), CO_2 does not ignite or explode; its toxicity (risk of asphyxiation) occurs at a much higher concentration in the air and its GWP and ODP data are much lower: for example, the GWP of propane is 3 while that of CO_2 is 1 by definition [32]. It boasts also a very high thermal resistance, which allows for a wide operation temperature range in power cycles, from for example 200 °C (including e.g., heat recovery cycles and geothermal applications [33]) up to 500 °C (including solar [34] and nuclear [35] applications). All these characteristics make CO_2 a versatile cycle fluid: while the usages of steam and air are limited respectively to Rankine and Brayton cycles, CO_2 can be used in both and, moreover, not only within power cycles but also within refrigeration ones.

Finally, the closed nature of these cycles results in rather clean circuits, apart from the need to stop wear particles by filtration. This contrasts with the complex and costly water treatment of steam cycles and the need of periodical cleanings of gas turbines due to the progressive fouling of their compressors by dust and salts from ambient air.

4.2. The Conceptual Drawbacks

4.2.1. Low Pressure Ratios Cause Low Specific Power Outputs

Although supercritical cycles operate at high pressures, they have low pressure ratios. Indeed, given that the pressure of a true supercritical cycle (Brayton) must exceed 73.8 bars in all stages, the pressure ratio ("Rc") turns out to be rather limited. For example, if we reasonably limit the value of P+ to 250 bar and start compression at P– = 75 bar, then the Rc is barely 3.3, leading to low enthalpy drops and limited expansion works in the power turbine.

In contrast, modern gas turbines boast Rc data ranging from 20 to 30. Although transcritical condensation (Rankine) cycles have P- values lower than 73.8 bar (Figure 1C), they are subject to a similar limitation because reducing P– too much would require increasingly colder heat sinks. Non-condensing transcritical cycles (called "dry transcritical" above) escape this limitation since P- can be set below Pc (Figure 1D): taking for example P– = 30 bar results in Rc climbing to 250/30 = 8.3. However, this is at the expense of complexity since there is need for additional compression/cooling sequences.

Low Rc values result in low turbine outputs. We can define the "specific power output" (SPO) of a power generation unit as its electrical output (W_{el}) divided by the mass flow rate (Q^m) of the fluid passing through the cycle, i.e., SPO = W_{el}/Q^m.

Table 1 compares, in their orders of magnitude, the SPOs of three usual cycles, namely: steam-Rankine; air Brayton and sCO_2 Brayton. The SPOs of the sCO_2 cycles turn out to be roughly 3 times (respectively 15 times) lower than that of an F-class gas turbine cycle (respectively of a steam cycle). Nevertheless, this does not prevent the reduction in equipment size mentioned above owing to the much greater density of supercritical CO_2.

Table 1. Compared SPO data of typical steam-Rankine, air-Brayton and sCO_2 Brayton cycles.

Cycle Type	Two-Pressure Steam Rankine	Air Brayton (F-Class Gas Turbine)	sCO_2 Brayton (RCBC)
Fluid	H_2O	Air & Comb. Gas	CO_2
T–/T+ [°C]	20/540	20/1350	45/550
P+/P– [-]	75/0.05	30/1.013	225/75
Rc (press. ratio)	1500	20	3
SPO = W_{el}/Q^m (1)	~1450	~300	~100

(1) the unit of SPO is kWe/($kgCO_2$/s) or kJe/$kgCO_2$.

4.2.2. Low Specific Power Requires Intense Heat Recuperation

As the turbine generates little power, it discharges still hot CO_2. Heat recuperation at its outlet, before heat rejection, is then desirable to improve efficiency. In other words, sCO_2 cycles require intense thermal recuperation.

4.2.3. The Narrow Operability of sCO_2 Rankine Cycles (Figure 1C)

The critical temperature of CO_2 is rather low (Tc = 31.1 °C). Consequently, heat sinks capable of completely condensing CO_2 must have a maximum temperature of about 25 °C. Unfortunately, such cold heat sinks are not so common and will become less available due to the global climate change, which is a strong handicap for sCO_2 Rankine cycles.

Two options can be explored to resolve this issue:

Option A—Attempts to increase the critical temperature [36,37]:

The first possible approach consists in looking for a substance "X" which, once blended with CO_2, would increase the Tc value by e.g., 15 °C. To keep the content of this article balanced, the studies made in that respect will be set out in Appendix A.

However, ultimately, these attempts show that it looks impossible in practice to find such molecule that would be acceptable from an EHS and cost standpoint.

Option B—Moving from a "wet transcritical" to a "dry transcritical" cycle:

The second approach consists in passing from a "wet transcritical" (i.e., Rankine) to a "dry transcritical" cycle (Figure 1D) since the latter does not impose any conditions on the heat sink temperature.

In fact, a "dry transcritical" cycles, as it is sketched in Figure 1D and in more detail in Figure 6, offers an interesting option to both address the narrow operability of the Rankine cycle (represented in Figure 1C) and improve the efficiency of a true supercritical cycle (Figure 1B).

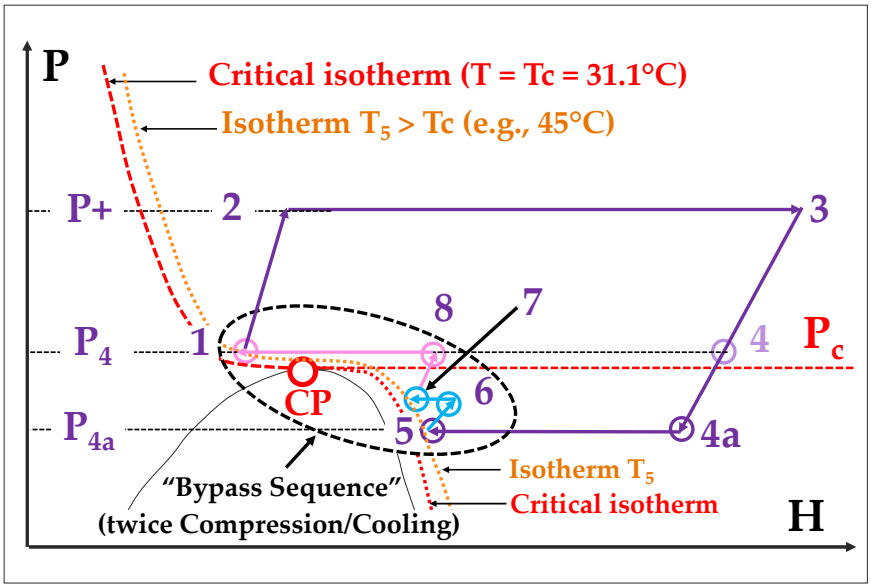

Figure 6. "Dry transcritical" cycle: the cooling stage is stopped when reaching the 45 °C isotherm.

In comparison with Figure 1B, the expansion stage 3 → 4 is extended below the critical pressure, up to a point 4a corresponding, for example, to P_{4a} = 30 bar. Then, compared to Figure 1C, the cooling stage is stopped when reaching an isotherm at a temperature slightly higher than Tc (for example at point 5 where T_5 = 45 °C)

A "bypass sequence"–here a double process of (compression/cooling)–replaces the condensation step of Figure 1C and allows to return to point 1 which is located on the T_5 isotherm. This cycle variant thus allows to expand the CO_2 below the CP and to close the cycle without crossing the condensation dome. It is transcritical by nature but remains "dry" since it is without condensation, which dispenses from a low temperature heat sink.

It has also two additional advantages from an efficiency point of view:

- The Rc value becomes increased from (P_3/P_4) to (P_3/P_{4a}): we thus escape the pressure ratio limitation suffered by true supercritical Brayton) cycles
- There are other improvements in efficiency, which again result from Equation (1); indeed, referring to the chart of Figure 3, the extended expansion causes the density to pass from about 75 kg/m^3 (point 4) to about 50 kg/m^3 (point 4a); moreover, ρ increases again during the recompression stages from point 5 to point 8.

This option has been actually exploited in the Allam cycle [3,38] as well as in Echogen's EPS 100 project [30,39].

However, a main drawback is the need for additional compression and cooling stage(s) to perform the bypass sequence. Additionally, it cannot be combined with the double recuperation/recompression cycle described below (§ 5.2), as it would generate excessive added complexity.

In conclusion, although sCO_2 transcritical Rankine cycles can be used in winter in cold and temperate climates, their operability is weak in summer and in hot climates. This is the main reason why they are not actually used for power generation, being more suitable for refrigeration applications.

This apparent impossibility to improve the operability of sCO_2 Rankine cycles is very detrimental to the deployment of the sCO_2 technology, because these cycles would have provided interesting performances in the field of heat recovery at low temperatures, where Brayton cycles are less efficient, as it will be shown in detail at § 6.2. This was the objective of the EPS100 project which seems however to have been interrupted.

Therefore, the rest of this article will focus on sCO_2 Brayton cycles.

4.2.4. The Gap between Conceptual and Practical Evaluation

The conceptual evaluation outlined above, shows very favorable thermodynamics but it relies on ideal conditions. In reality, the actual isentropic efficiencies of turbomachines have a strong impact on performances. Moreover, the technology of sCO_2 power cycles is sometimes said to be in its "infancy" [40] and there is still progress to be made to reach optimized performances. The technical aspects of this topic, which are rarely covered in the academic literature, will be tentatively addressed in Section 7.

However, before tackling these engineering aspects, we need to provide a description of the possible architectures for sCO_2 Brayton cycles and assess their respective performances.

5. Outstanding Architectures of sCO_2 Brayton Cycles

As already stressed, sCO_2 cycles require intense heat recuperation to compensate for the low compression ratios and limited outputs of the power turbine. Therefore, we will omit non-recuperated cycles (denoted as "option 0") and will focus on the most promising architectures.

In doing so, we will use the following inputs: (T–, T+) = (45, 550 °C) and (P–, P+) = (75, 225 bar) corresponding to an Rc of 3; the pinch temperatures of heat exchangers are 10 °C.

5.1. Architecture 1: Simple Thermal Recuperation (or "Simple Cycle" Configuration)

Figure 7 shows a sketch of a 20 MWe Brayton sCO_2 cycle that comprises a CO_2 heater (H) and a single recuperator (R). The corresponding P-H diagram is presented in Figure 8 [41].

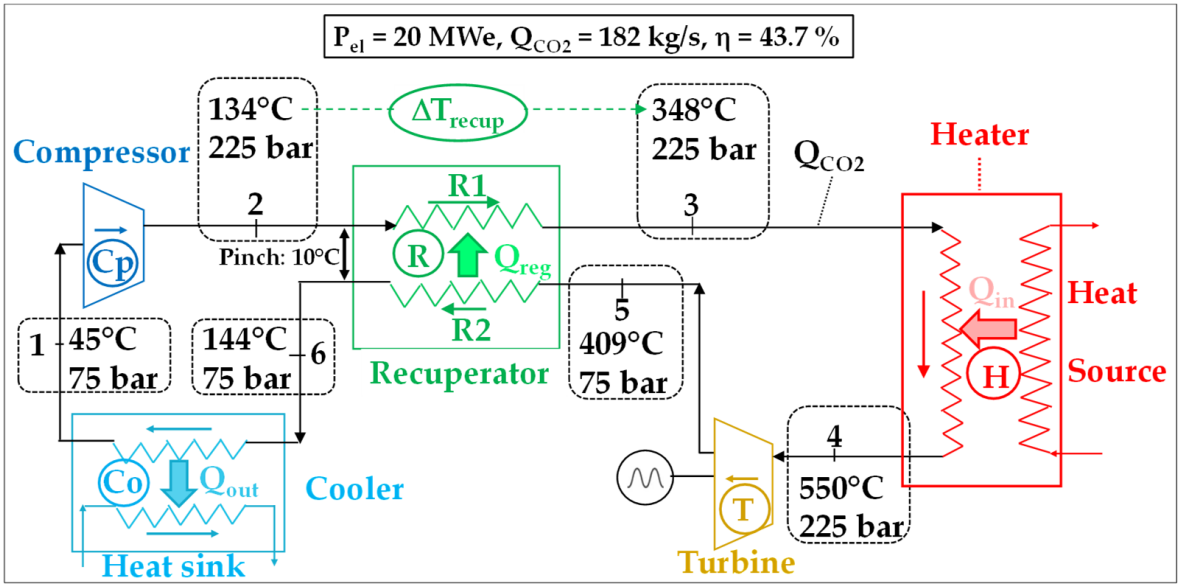

Figure 7. Flow diagram of a "simple recuperation architecture"; performance in "ideal" conditions.

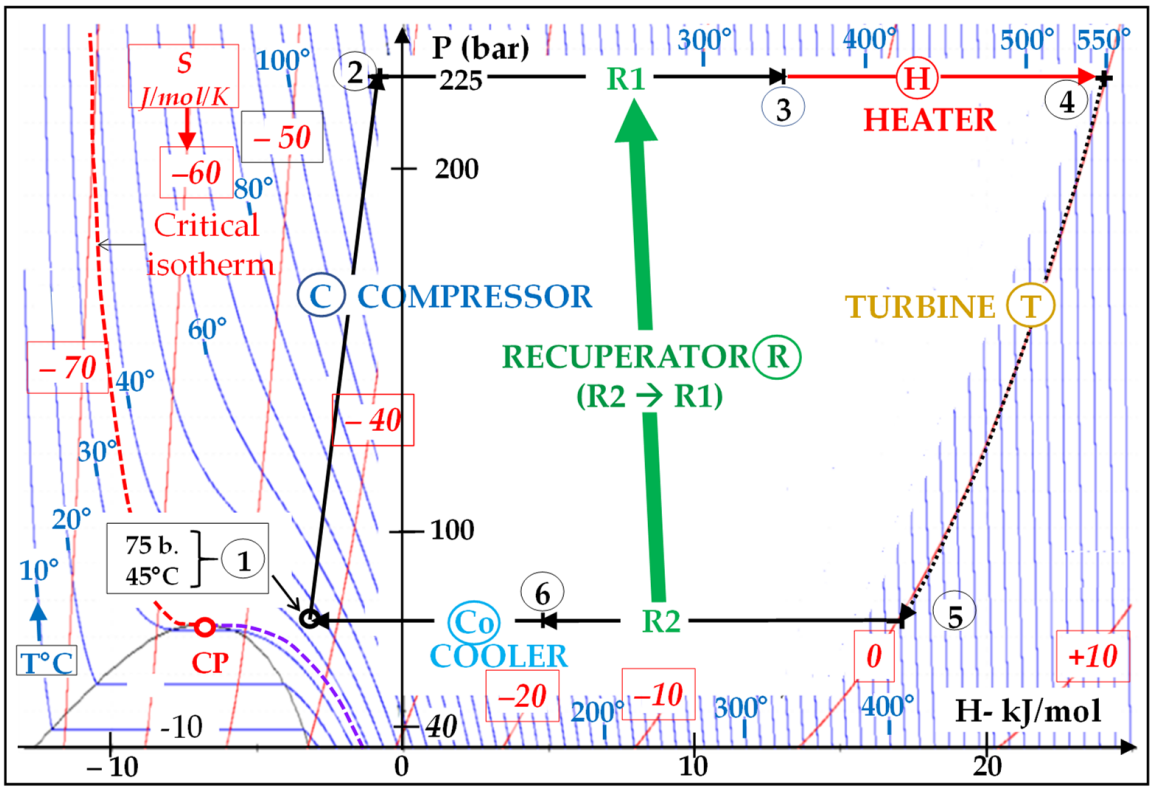

Figure 8. P-H diagram of the simple-recuperated Brayton cycle (architecture 1).

The recuperator R transfers some heat from the hot, LP branch (mark R2) to the colder, HP branch (mark R1) of the cycle. Doing so, the HP CO_2 stream has its temperature increased by an amount noted "ΔT_{recup}" before it enters the heat source, which diminishes the heat to be extracted from the latter.

This configuration is sometimes called "simple cycle" owing to the use of a single recuperation.

The results of the thermodynamic simulation (listed in Figure 7) indicates that the CO_2 through-flow necessary to generate 20 MWe is 182 kg/s, which corresponds to an SPO of 110 kJe/kgCO_2.

The heat recovery rate is truly considerable since the temperature increases by $\Delta T_{recup} = T_3 - T_2 = 214$ °C at the entrance to the heat source.

The thermodynamic simulation shows that the intrinsic electric efficiency of this simple-recuperated sCO_2 cycle is $\eta_{intr} = 43.7\%$.

It would be reduced by more than half, falling to 20%, if we removed the recuperator, which would be the "option 0" that is in fact never used due precisely to its very poor efficiency.

Back to the size reduction effect:

As mentioned above, the cross-section of a turbomachine is sized to be proportional to the volumetric flow (Q^v in m^3/s) of the fluid, or-which is equivalent-to the ratio between its mass flow rate (Q^m in kg/s) and its density (ρ in kg/m^3).

Table 2 compares the sizes of (i) the 20 MW sCO_2 turbine involved in the "simple cycle" architecture above and (ii) a conventional 20 MW steam turbine (ST).

The steam turbine has both an HP and an LP casing. The comparison is made at turbine discharge where the gas speed is greatest. The calculation shows a diameter twice greater for the HP steam casing and about 12 times greater for the LP steam casing.

Despite these substantial gains in efficiency and size, this *architecture 1* faces an efficiency limitation, which comes from the fact that the heat capacity (Cp) of supercritical CO_2 decreases significantly when its pressure decreases, as illustrated by Figure 9 [28].

Table 2. Comparative sizes of a steam and a sCO_2 turbine.

sCO_2 Option: sCO_2 turbine/single casing-Q^m = 182 kg/s	**Steam Option:** Steam turbine with 2 casings: HP casing-simple flow-Q^m = 36.2 kg/s LP casing-dual-flow-Q^m = 36.2 kg/s	**Steam/sCO_2 diameter ratio =** $[(Q_{steam}/Q_{CO_2})/(\rho_{H_2O}/\rho_{CO_2})]^{0.5}$
409 °C, 75 bar: ρ_{CO_2} = 57.4 kg/m^3	HP: 208 °C, 5 bar: ρ_{H_2O} = 57.4 kg/m^3	2.3
	LP: 45 °C, 0.1 bar: ρ_{H_2O} = 0.077 kg/m^3	11.7

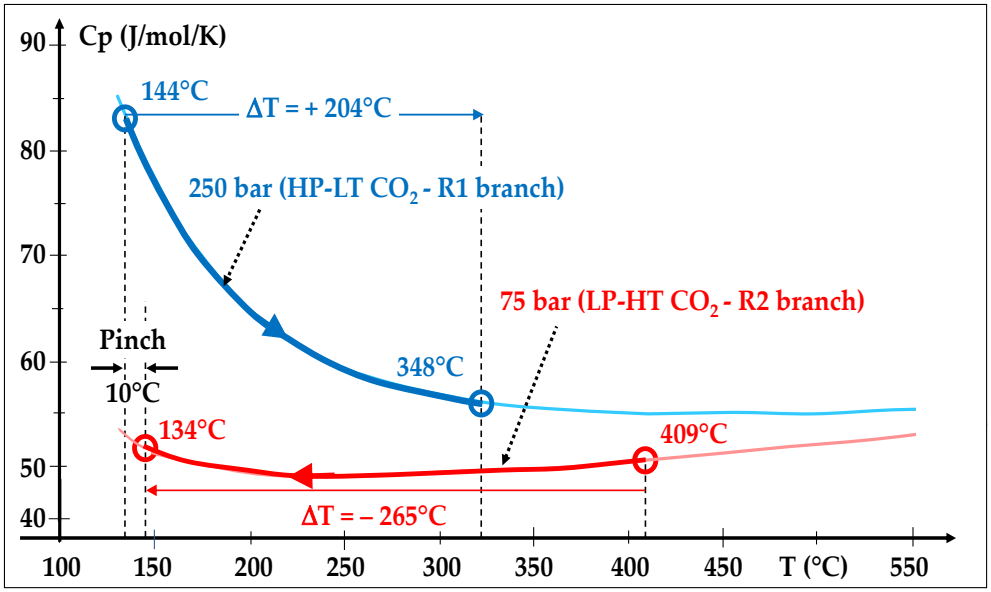

Figure 9. Heat recuperation: the dissimilar Cp in the two branches unbalances the heat exchange.

Indeed, the cold CO_2 stream in the HP branch (R1) has a higher Cp than the hot CO_2 stream in the LP branch (R2). This causes an unbalanced temperature profile inside the recuperator. More precisely, we can observe in Figures 7 and 9 that the HP CO_2 stream heats by only 204 °C (348–144) while the LP CO_2 stream cools by 265 °C (409–144).

5.2. Architecture 2: Double Recuperation and Recompression (Recompression Closed Brayton Cycles or RCBC)

To overcome this limitation, we can create a second exchange between the HP and LP CO_2 streams, which however requires recompressing a fraction of the LP-CO_2 to inject it into a second recuperator (Figure 10) [42].

To do this, the stream of CO_2 leaving the first recuperator (the "LT" one) is divided, at point P, between the cooler (mark Co) and a "recompressor" (mark RC), using a three-way valve (V) which provides a variable flow splitting ratio. This recompressed fraction "x" is injected into the HP branch of a second recuperator (the "HT" one).

To designate this new cycle architecture, we will adopt, in the rest of this article, the expression "Recompression Closed Brayton Cycle", and more shortly the acronym "RCBC" to comply with the most widespread use.

The inputs (T–; P–; T+; P+ and pinches) used in the simulations are unchanged. To produce again 20 MWe, the main CO_2 flow (crossing the turbine) must be 200 kg/s (i.e., an SPO of 100 kJ/kgCO_2) and the optimum "recompressed flow" must be 47.8 kg/s, corresponding to fraction x = 0.239.

The main results are reported in Figure 10. The intrinsic electric efficiency η_{intr} is 48.3%, which is 4.6 points more than in *architecture 1*.

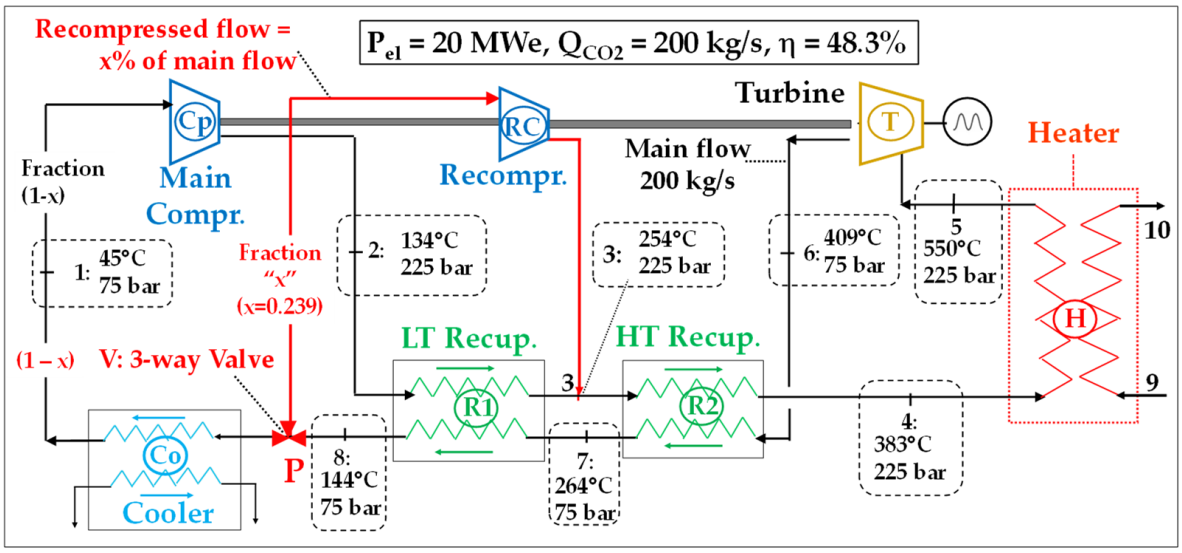

Figure 10. Flow diagram of a double-recuperation, recompression sCO_2 cycle; "ideal" conditions.

It is therefore clear that the RCBC variant significantly improves the heat recovery process as we have: $\Delta T_{recup} = T_4 - T_2 = 249$ °C (versus 204 °C in architecture 1), providing thus 4.6 additional points of efficiency. This efficiency level honorably compares with most modern simple-cycle gas turbines that are fired at 1400–1500 °C. As a result, RCBC cycles outperform, above 550 °C, all other cycles operating with similar heat source temperatures (Figure 11) [43,44].

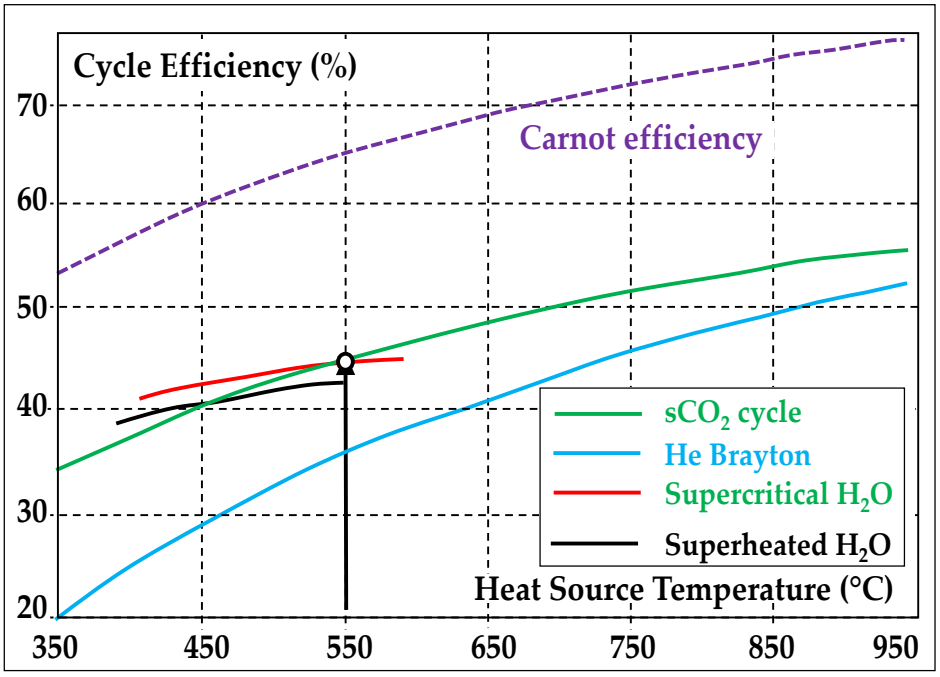

Figure 11. Compared efficiencies of sCO_2, Helium and Superheated/Supercritical H_2O cycles; Common comparison basis: "ideal conditions"-heat sink taken at 15 °C; after [44].

However, this comes at the expense of the simplicity of the cycle.

5.3. Other Possible Architectures

Architectures 1 and 2, which involve a single CO_2 heater, are of interest in applications where the heat source is at a fairly constant temperature and its heat can be easily extracted

using a single heater and a heat carrier (at best a liquid) that circulates in the hot branch of the heater (line 9–10 of Figure 11). This is the case (i) in solar units, e.g., in CSP plants using molten salt as heat carrier, with heat source temperatures ranging from 500 to 700 °C [45] and (ii) in nuclear units, namely in Small Modular Reactors (SMR) having turbine inlet temperatures in the range of 500–600 °C [46].

However, other architectures are possible [47]. Some of them involve two or more CO_2 heaters which become necessary when the temperature window of the recuperation is too wide to be accommodated by a single one. An important example is the recuperation of residual heat from combustion gases, released e.g., by diesel engines or gas turbines. Such an example is covered below (§ 6.2).

6. Two Paradigmatic Applications: Solar Power and Heat Recovery from Hot Gases

In this section, we will illustrate the performances of RCBCs through two important applications. This time, to carry out a closer assessment of the merits and limitations of sCO_2 Brayton cycles, we will assess their performances not only in "ideal" but also in "realistic" conditions.

6.1. Concentrated Solar Power Plant (CSPP)

Figure 12 represents a typical CSPP [48,49]. Solar energy is reflected by a field of heliostats towards a receiving tower which constitutes the heat source. The heat is extracted by a molten salt (often a eutectic mixture of alkaline nitrates). This heat carrier is stored in a hot tank; it feeds a steam generator, which powers in turn a Rankine cycle and is then collected in a "cold" tank from where it returns to the receiving tower.

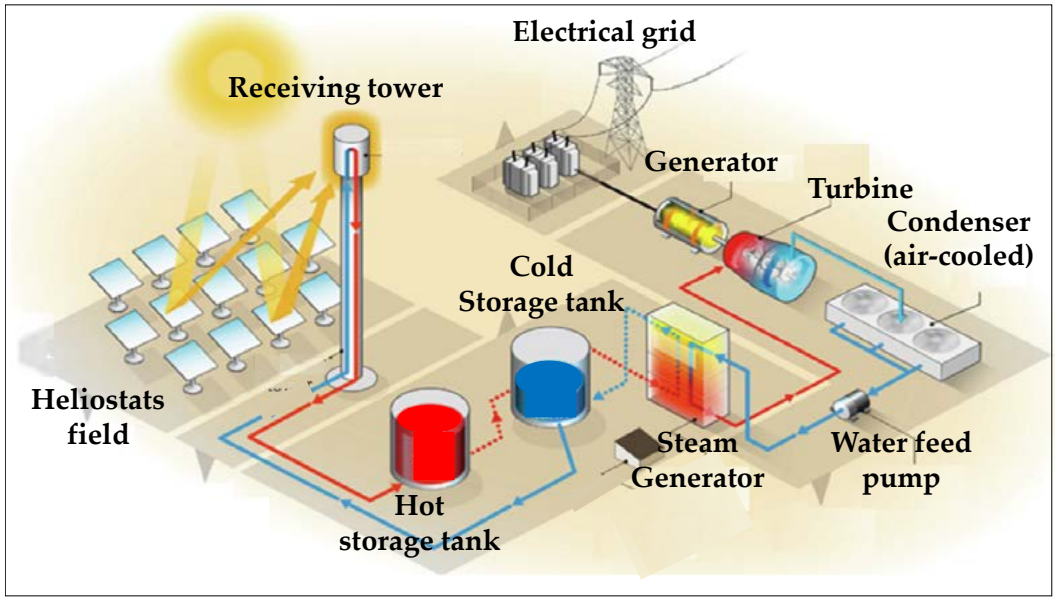

Figure 12. Sketch of a typical CSPP equipped with a steam Rankine cycle, after [48].

The typical Rankine cycle is sketched in Figure 13, with the data of the main streams.

It has both superheat (176 bar-552 °C) and reheat (42 bar-551 °C) stages. The heat sink (an air-cooled condenser) is taken at a temperature (T–) of 45 °C which is the condensation temperature of the cycle. The molten salt enters the receiving tower at 565 °C with a flow rate of 324 kg/s and leaves it at 290 °C (the minimum temperature to keep it above the solidus of the salt): there is an exchange of 270.3 MWth in the steam generator. The approach temperature is 13 °C. In these conditions, the "ideal" power output is 119.3 MWe and the efficiency 44.1%; the overall steam flowrate is 226 kg/s with an SPO of 528 kJe/kg.

"Realistic" performances are obtained using a value of 92% for the average isentropic efficiency of the whole steam turbine (values vary from 90 to 95% between the HP, MP and

LP casings); the contributions of water pumps are negligible. The actual power is then 109.8 MWe and the efficiency is 40.6%.

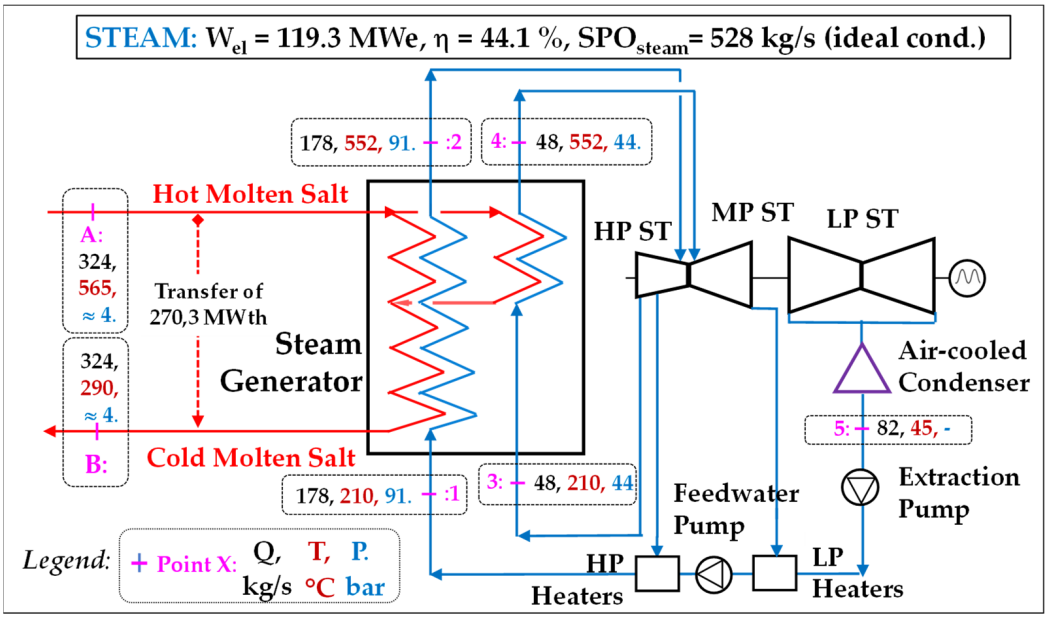

Figure 13. The two-pressure steam Rankine cycle used for the CSPP; operation in "ideal conditions".

6.1.1. Transposition into an sCO_2 Brayton Cycle

The "candidate" Brayton sCO_2 cycle which is chosen to challenge the above Rankine cycle is of the RCBC type as described in § 5.2. It is fed with the same molten salt at 565 °C and exchanges also 270.3 MWth with it. Its evaluation was carried out with the same input data as before: T– = 45 °C and P– = 75 bar.

Figure 14 shows such possible transposition and the results of a corresponding simulation performed firstly in ideal conditions.

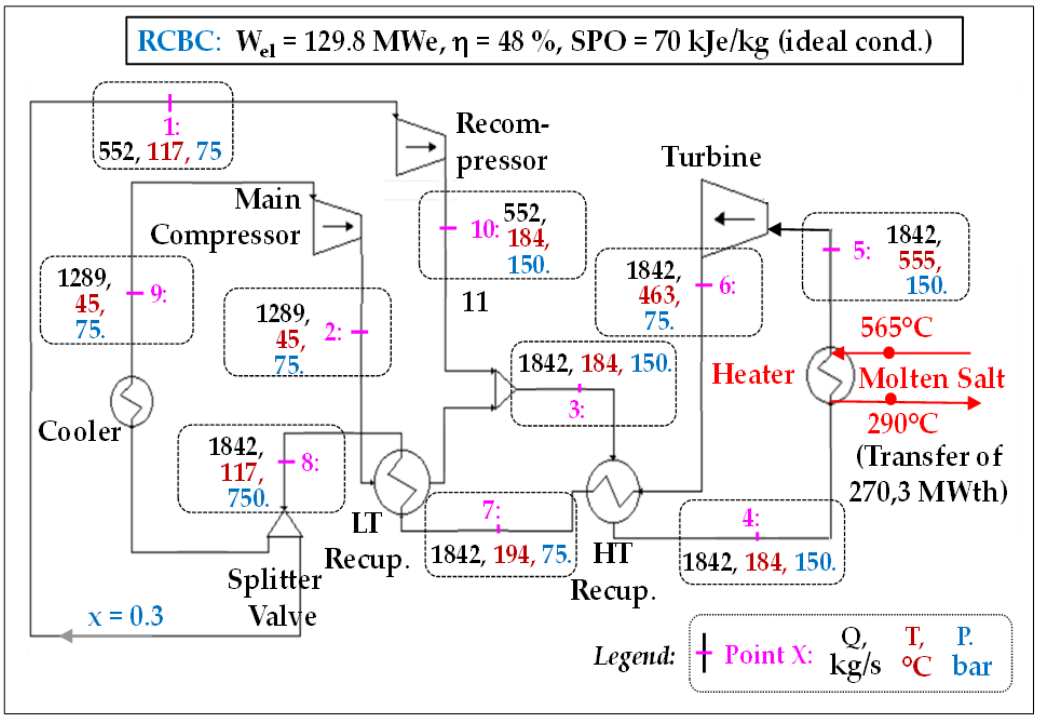

Figure 14. Possible RCBC cycle to power the CSPP; performance in "ideal" conditions.

The optimum efficiency is reached with the following parameters:

- main CO_2 flow Q_{CO_2} = 1842 kg/s
- P+ = 150 bar (i.e., a compression ratio Rc of only 2)
- recompression fraction: 30%.

We have also calculated the "realistic" performances, for which we have taken typical isentropic efficiencies of 0.90 for the turbine and 0.85 for the compressors (instead of 1). These values are slightly higher than those retained as objectives in the STEP program (see § 7.1).

6.1.2. Simulation Results of the Candidate sCO_2 Cycle and Short Discussion

The efficiency assessed in "ideal" conditions is 48% and the power output is 129.8 MWe: we thus observe a gain of 3.9 points in efficiency compared to the Rankine cycle equipped with superheat and reheat. The SPO is however much lower: 70 kJe/kgCO_2.

Nevertheless, in "realistic" conditions, the net power drops to 108.3 MWe and the efficiency to 40%: the RCBC loses 8 points and goes to 0.6 point below that of the steam Rankine cycle (40.6%).

This mediocre result is mainly explained by the fact that the water feed pump of the Rankine cycle is incomparably more efficient than the CO_2 compressors despite the supercritical state of the latter fluid, as it has been already highlighted in § 4.1.1 and illustrated by Figure 3.

6.2. An Important Application to Reduce Carbon Footprints: Heat Recovery from Combustion Gases

This paragraph deals with the recovery of residual heat carried in the flue gases of a thermal equipment, for example a gas turbine (GT) [50]. The whole (GT + recovery cycle) will then constitute a Gas Turbine Combined Cycle (GTCC), the GT representing the "topping" cycle [51] and the recovery cycle being the "bottoming" one [52,53]. Incidentally, we can notice that this sCO_2 application profile is identical to that developed in Echogen's EPS100 project, which employed however an sCO_2 Rankine cycle [30,39].

In applications of this type, it is necessary to use several heat exchangers to maximize heat recovery. Indeed, the temperature of the flue gases decreases as the exchange progresses and the operator's goal is of course to reduce it as much as possible (for example from 550 to 70 °C), in order to maximize the overall efficiency of his GTCC.

Our goal is to see whether an sCO_2 design can become a "challenger" for a two-pressure steam cycle which is the "title order" in contemporaneous industrial GTCCs [53]. We will then simulate both cycles and compare their performances. This comparison will be carried out in "ideal" conditions and the transition to "realistic" conditions will then be discussed.

The gas turbine is an E-class machine which is fired at a temperature in the range of 1100–1150 °C and generates an output ($W_{el,GT}$) of 122.1 MWe, with an electrical efficiency of 33.4%. Its heat consumption is Wth_{GT} = 122.1/0.334 = 365.6 MWth (on a fuel LHV basis). The maximum Recoverable Heat is then RH_{max} = ($Wth_{GT} - W_{el,GT}$) = 243.5 MWth; this heat is carried by a flow of 412 kg/s of combustion gases ("cg") that are released at 544 °C.

6.2.1. Design of the "Candidate" sCO_2 Cycle

The candidate sCO_2 cycle is again of the RCBC type, the most efficient.

However, this time there is both an HT CO_2 heater and an LT CO_2 heater which capture heat respectively on the hot zone and the cold zone of the flue gas stream (Figure 15). They are associated with an HT turbine and an LT turbine, respectively. The ratio between the flows of CO_2 directed towards the HT and LT heater is adjusted via a splitter valve V2. The low temperature of that cycle (T–) is again 45 °C and its pressure P– is again 75 bar.

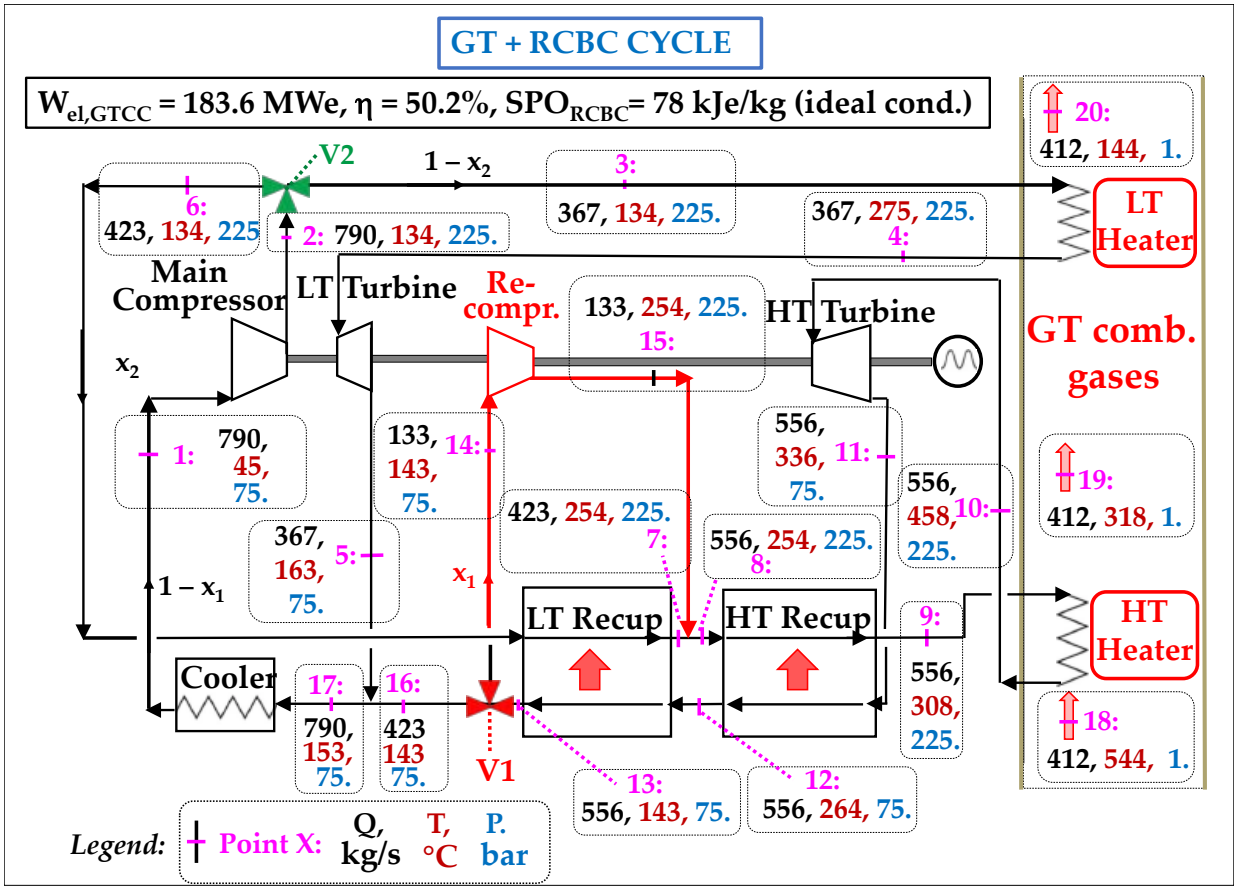

Figure 15. Sketch of the sCO_2 heat recovery cycle (architecture 3) with two CO_2 heaters and two power turbines.

This leads to an "*architecture 3*" of sCO_2 cycle. Thermodynamic simulations performed in ideal conditions and including a sensitivity study, show that the optimal electrical efficiency is obtained with the following parameters:

- main CO_2 flow: Q_{CO_2} = 790 kg/s: it is the flow crossing the main compressor
- fraction of recompressed flow: x_1 = 133/423 = 0.31
- flow splitting between the LT and HT heater: x_2 = 367/423 = 0.87.

These optimized operating parameters lead to an electrical power output W_{el,sCO_2} of 61.5 MWe for this RCBC of *architecture 3* and an intrinsic electrical efficiency (η_{intr}) of 33.7%. We notice that this value is significantly lower than that (48%) we had obtained with *architecture 2* (§ 4.2) which involved a single heater and a similar initial (but constant) heat source temperature (550 °C). The heat actually recovered by the two recuperators is $RH_{actual} = [H_{cg}(544\ °C) - H_{cg}(144\ °C)]$ and is equal to 182.5 MWth; the "heat transfer rate" (η_{trans}) is thus RH_{actual}/RH_{max} = 182.5/243.5 = 75.0%.

The net conversion efficiency (η_{net}) of this sCO_2 cycle is therefore $\eta_{net} = \eta_{trans} \times \eta_{intr}$ = 0.337 × 0.75 = 0.253: it is the ratio between the electrical power generated by this cycle and the maximum recoverable heat. The temperature of the flue gases downstream of the LT heater is 144 °C, because the CO_2 enters it at 134 °C and the pinch temperature is 10 °C.

The specific power output is then $SPO = W_{el,sCO_2}/Q_{sCO_2}$ = 61,500/790 = 78 kJ/kgCO_2: it is lower than those found with the previous architectures (around 100 kJ/kgCO_2).

Finally, it is interesting to deduce the electrical power of the overall GTCC: $W_{el,GTCC} = W_{el,GT} + W_{el,sCO_2}$ = 122.1 + 61.5 = 183.6 MWe and its efficiency, which is equal to that power output divided by the heat input of the GT: $\eta_{GTCC} = W_{el,GTCC}/Wth_{GT}$ = 183.6/365.6 = 50.2%.

6.2.2. Design of the Reference Steam Rankine Cycle [53]

The recovery cycles in GTCCs are classically subcritical, two-pressure steam cycles (for example: 70 bar-520 °C/5 bar-210 °C). We will consider such one exploiting the same residual heat stream. Figure 16 shows the corresponding diagram along with the properties of H_2O at the main cycle points.

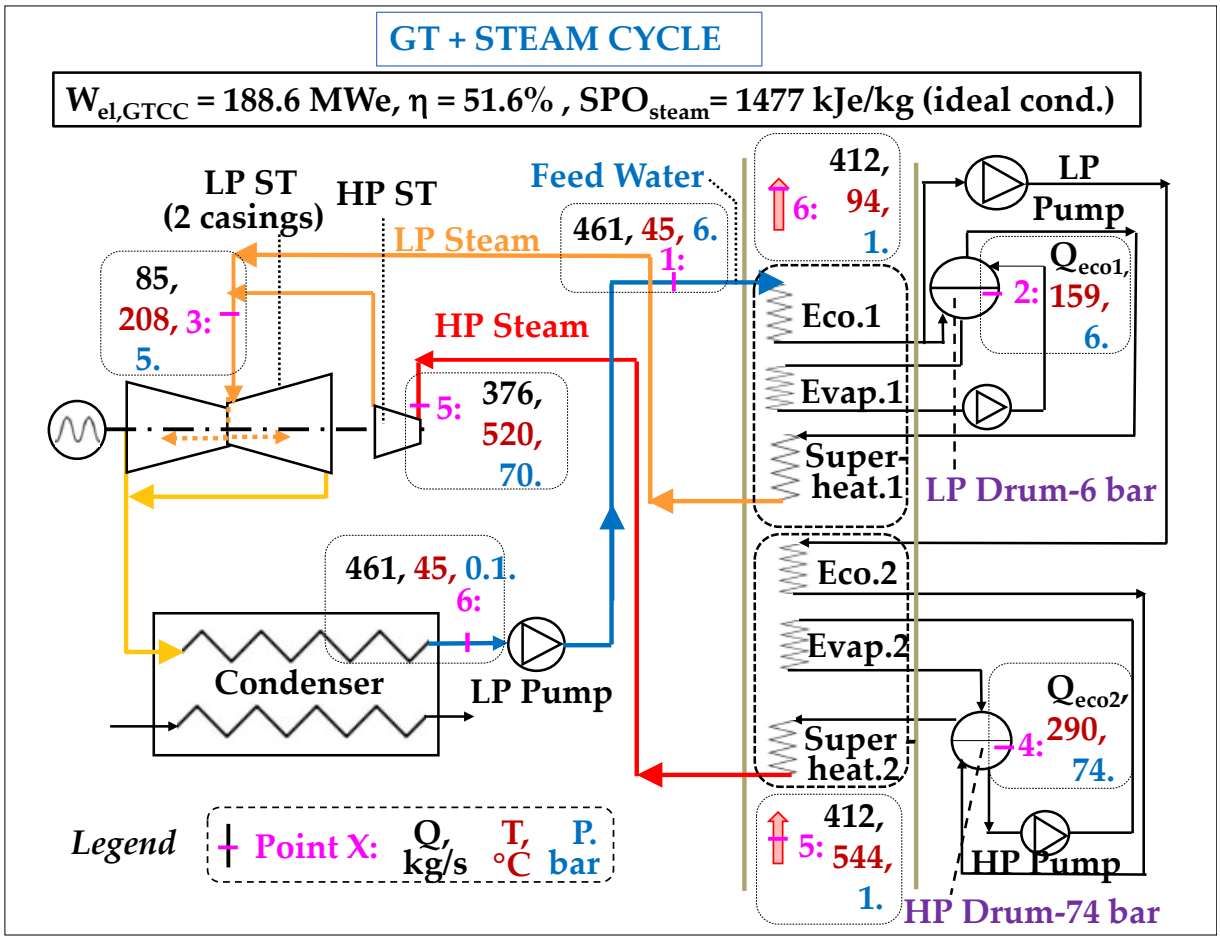

Figure 16. Sketch of the two-pressure, Rankine recovery cycle; ideal conditions.

The calculations in ideal conditions show that the power output of this steam cycle is $W_{el,steam}$ = 66.5 MWe. Its net conversion efficiency is therefore $\eta_{net} = W_{el,steam}/RH_{max}$ = 66.5/243.5 = 27.3%. The specific power output of this steam cycle is SPO = $W_{el,steam}/Q_{steam}$ = 66,500/45 = 1477 kJ/kg of steam, a value much higher than for the sCO_2 cycle (78 kJ/kg of CO_2).

The temperature of the combustion gases released into the atmosphre (at the outlet of *Economizer No. 1*) is 94 °C, significantly lower than the corresponding value in the sCO_2 version (144 °C). The heat which is actually transferred to the steam cycle is then $RH_{actual} = (H_{cg}(544\ °C) - H_{cg}(94\ °C))$ = 202.8 MWth and the intrinsic electrical efficiency is $\eta_{intr} = W_{el,steam}/RH_{actual}$ = 66.5/202.8 = 32.8%.

The heat transfer rate (η_{trans}) is RH_{actual}/RH_{max} = 202.8/243.5 = 83.3%, which is remarkably high.

Finally, the total power of the resulting GTCC is 122.1 + 66.5 = 188.6 MWe and its efficiency is $\eta_{GTCC,steam} = (W_{el,GT} + W_{el,steam})/Wth_{GT}$ = 188.6/365.6 = 51.6% in ideal conditions.

6.2.3. Discussion

This comparative study between the performances of an RCBC and a two-pressure Rankine cycle operating in ideal conditions, within a multiple heat recovery application, calls for the following discussion.

- Intrinsic efficiencies

The intrinsic efficiency of the sCO_2 cycle exceeds that of the steam cycle by nearly 1 point (33.7 versus 32.8%). This is essentially because the steam cycle rejects much heat (the totality of the condensation heat of CO_2) to the heat sink.

- Global performance

However-and this is the most important result-the steam cycle quite significantly outperforms the sCO_2 cycle, by 2 points, in terms of overall efficiency: 27.3 versus 25.3%. This translates into a better efficiency of the GTCC using the steam-based bottoming cycle: 51.6% versus 50.2%.

- What are the reasons for the success of the steam cycle?

The superiority of the two-pressure steam cycle in this multiple heat recovery application is mainly due to a much better heat transfer (η_{trans}) which is 83.3%, compared to 75.0%. Indeed, in the steam cycle, H_2O enters the economizer No. 1 as a low temperature liquid (45 °C: point 1 of Figure 16), while in the sCO_2 cycle, CO_2 is significantly hotter (134 °C: point 3 of Figure 15) as it has been previously compressed to 225 bar. In other words, while the pumping of water generates virtually no entropy and no temperature increase, on the contrary, the compression of CO_2 significantly increases its temperature despite its supercritical state: this increase here is by 89 °C in the main compressor and by 111 °C in the recompressor. This remark once again highlights the importance of Equation (1) set out in § 4.1.1, knowing that the density of liquid water (about 1000 kg/m^3) is about twice higher than that of supercritical CO_2 (400 to 600 kg/m^3 along its compression stage: Figure 3); moreover, in Equation (1), the molecular mass of H_2O is about 2.5 times lower than that of CO_2.

However, one can argue that, since the steam cycle employs a greater number of heat recovery exchangers (6 versus 2), increasing their number in the sCO_2 cycle would suppress that efficiency gap. In fact, this is not the case because one could not have a CO_2 temperature lower than 134 °C at the inlet of these LT exchangers, so that the overall heat recovery efficiency would not improve significantly.

Another a priori possible way to improve the efficiency of the sCO_2 architecture would be to equip the compressor with an intercooler which would lower the temperature at the inlet of the LT heater and improve the transfer rate in the latter. However, the additional calories thus recovered would only compensate for those lost in the intercooler.

In summary, the better heat recovery achieved by H_2O highlights the interest of using a liquid cycle fluid in the low-temperature portion of a cycle and, more generally, in low-temperature recovery applications.

Overall, the performance of Brayton sCO_2 cycles proves limited in the field of low temperature heat recovery, essentially due to (i) the impossibility of having, after compression, a CO_2 carrier at a temperature below, say, 100 °C to maximize heat capture and (ii) the need for a relatively high number of turbomachines which destroy considerable amounts of exergy; in this example, four of them are used: two compressors and two turbines.

In this regard, it is really detrimental that the sCO_2 Rankine route is hampered by its insufficient operability, as it would more efficiently challenge the steam option, since the use of colder, liquid CO_2 would enable capturing significantly more heat at the LT heater and would give higher flexibility for alternative design variants as it is the case with H_2O.

6.3. Conclusions of the Two Comparative Studies

We have assessed RCBC cycles in two types of paradigmatic applications.

6.3.1. RCBCs Operated with Hot Heat Sources

- RCBC fired with heat sources at say 550 °C or more have a strong efficiency potential which raises them to the first place, before all conventional cycles operated at similar temperature (T+) levels.
- However, this advantage vanishes when one considers not ideal but more realistic performances of turbomachines, using levels of isentropic efficiencies congruent with those currently planned in sCO_2 development projects.

6.3.2. RCBCs Operated in Heat Recovery Mode with Multiple Heat Exchanges

- The heat recovery rate achieved by supercritical CO_2 in multiple heat recoveries is lower than that achieved by liquid H_2O (75% compared to 83.3% in our study)
- Moreover, in comparison with the steam cycle and despite the supercritical state of CO_2, there is a greater destruction of exergy especially during the pressure increase stages. This handicap is magnified by the need to use of two compressors. Incidentally, the exergy destruction is greater in the recompressor than in the compressor, because, in the former, the intaking CO_2 is hotter and less dense than in the latter.
- Finally, the handicap of the sCO_2 cycles would be significantly increased if we compared the performances no longer in ideal conditions but in more realistic conditions, using realistic isentropic efficiencies of turbomachines (significantly lower than 1).

In both applications, a significant jump in turbomachine performances appears necessary to improve the ranking of sCO_2 Brayton cycles and fully express the potential of this technology.

7. What Are the Challenges Posed by the Industrialization of sCO_2 Power?

At this stage, it is time to try to understand the reasons for the relatively slow industrialization process of sCO_2 cycles.

In this study, the comparison between RCBCs and steam cycles set out above will be important to quantify the progress to be made in turbomachinery if we want to see sCO_2 competing with conventional cycles and becoming active in the energy transition.

As pointed in the introduction, the foundations of the sCO_2 technology were established at the end of the 1960's and, since then, numerous development programs have been deployed worldwide to transpose it into industrial prototypes, first in the low power range and, more recently in a larger range.

Despite obvious progress, these efforts have not yet resulted in industrial designs allowing the release of medium to large power units. Amazingly, this delay is little discussed in the academic literature, probably due to the high engineering rather than purely scientific content of this subject. This situation contrasts with the great number of non-applicative publications devoted e.g., to cycle architectures variants.

In fact, most of the relevant information available on the actual experimental progress comes from a limited number of technical reports written by the developers themselves [30,39,54,55]. These reports contain complex and very specialized engineering considerations. In this context, the present discussion does not pretend to provide an authoritative view about the progress of the technology. It is rather an attempt–as objective as possible–to identify and document the underlying technological locks and challenges, relying on the (scarce) published information. Figure 17 summarizes some key stages of developments carried out to date and planned for the future. Only most important ones are reported as several other programs have been/are conducted namely on small scale units [24]. The STEP (Supercritical Transformational Electric Power) program represents the most coherent and continuous industrialization effort. It started in 2016, being subsidized by the US DOE and conducted the US GTI, the SwRI and GE as lead partners.

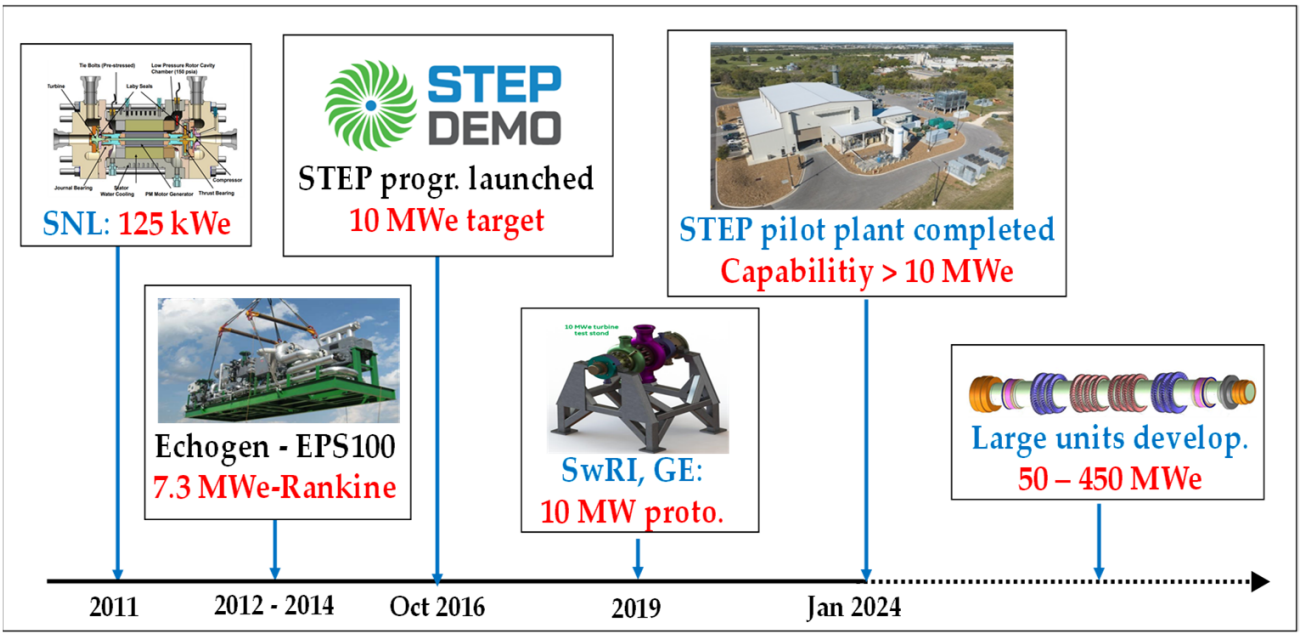

Figure 17. Some marking development milestones of the sCO_2 power technology.

The following analysis focuses primarily on what can be considered the critical aspects of a RCBC designs, which represents the most promising sCO_2 cycle architecture.

7.1. Basic Design Options Put Forward for sCO_2 Power Plants of the 50–450 MWe Classes

The discussion below will deal with the technology of turbomachines since these components represent the stumbling block of any sCO_2 cycle development program. It does not attempt to trace the detailed progress in the development of industrial sCO_2 prototypes, which began in the mid-2010s, mainly with funding from the US DOE, and is moreover subject to intellectual property rights. The objective here is rather to illustrate the strong design specificities of these components by referring to a few selected examples of preliminary concepts already published.

A first complication encountered during the development of large sCO_2 turbomachines regards the extrapolation of designs from the low- to the high-power range. Small turbomachines accommodate for high speeds (several tens of thousands of rpm). In contrast, larger ones require limited rotation speeds (e.g., 3600 rpm in the USA and 3000 rpm) because of much larger centrifugal forces acting on the blades and the rotor disks, due to higher masses and moments of inertia; incidentally, other considerations are relevant, including the "velocity triangle" and the feasibility of synchronization with the grid.

A first series of such preliminary concepts for turbomachine components was published in 2016 in two articles [54,55], at the end of the SunShot program and with the perspective of devising large industrial units (up to 450 MWe). In that study, the announced isentropic efficiency targets were as follows: 90.6% for the power turbine; 83% for the main compressor and 80.1% for the recompressor.

These articles proposed an ingenious concept in which the rotors of the turbine (3 HP + 3LP stages), the main compressor (radial; two-stage) and the recompressor (radial; four-stage) are all assembled on a single shaft.

Figure 18 shows this arrangement as well as notional geometries for the high- and low-pressure blades of the turbine.

The turbine was devised to be axial with symmetric dual-flow, like LP steam turbines of that power class. The compressor and recompressor were instead devised centrifugal (or "radial") which is made possible by the limited compression ratio needed, knowing that radial compressors can achieve higher compression ratios per stage than axial ones, thus occupying less axial length on the shaft.

Looking at Figure 18, we are surprised by:

- the very short length (less than 7 m) of the space occupied by the turbine rotor section, compared to conventional steam and gas turbines constructions
- the quite homogeneous geometry of the turbine blades along the different stages and their "lilliputian" sizes, these two points being explained by the low compression ratio, the high density and the low compressibility factor of supercritical CO_2.

We are also struck here by the minute axial lengths occupied on the shaft by the two rotors of the compressors; the reason for the larger dimensions of the recompressor is that it admits hotter, less dense CO_2.

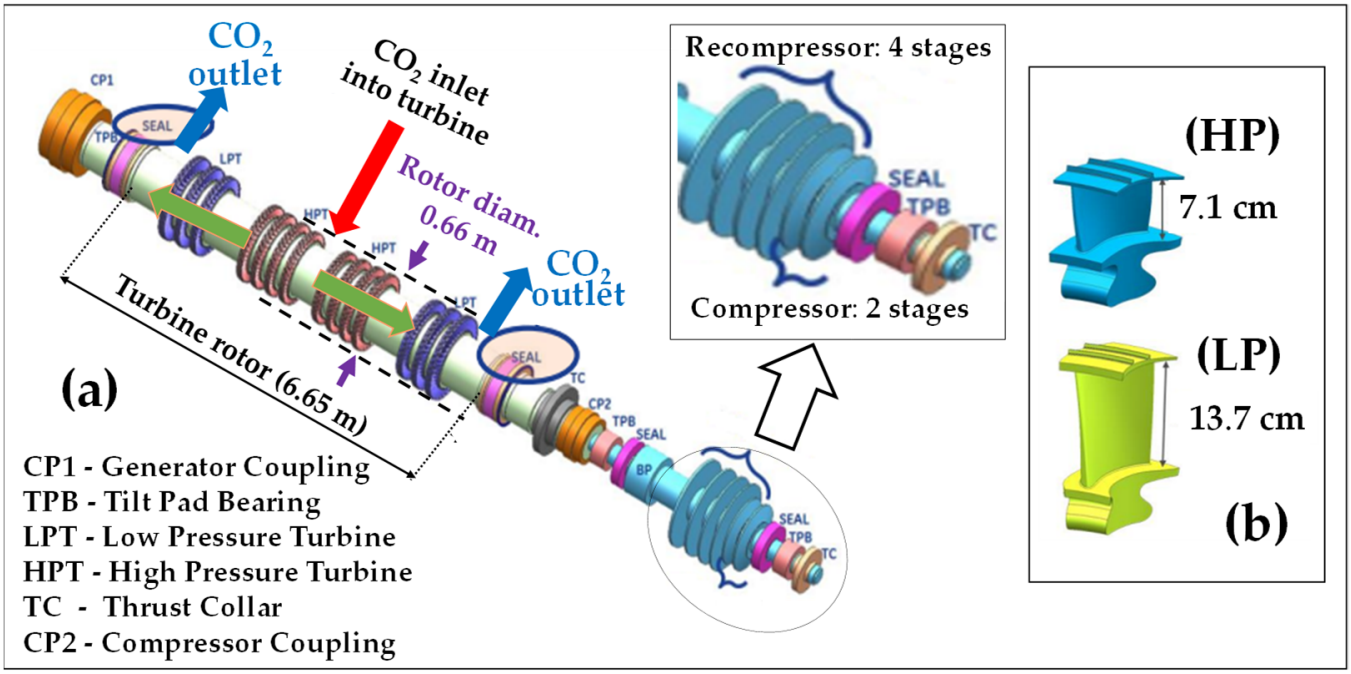

Figure 18. Study of Turbine-Compressor-Recompressor rotor for a 450 MWe class prototype (DOE's SunShot program): (**a**) Shaft; (**b**) Blades; with slight modifications and permission [54,55].

These design features therefore contrast radically with those of large contemporary steam and gas turbines. In the latter, rotor diameters are large due to high spatial velocities and they increase when pressure decreases, as a result of the low densities and important compressibility of the cycle fluids (steam and air/combustion gas, respectively). These features disappear in the case of a supercritical fluid which is both dense and very little compressible.

Figure 19 shows another concept of a 10 MW sCO_2 turbine that has been developed by the SwRI and GE, also under DOE's Sunshot Program [56].

It is an axial, four-stage machine that has successfully generated 15 MW gross power at 715 °C-250 bar (inlet conditions).

Here, the shaft diameter is very thin (76 mm) and the blade heights are very small and also virtually constant along the four stages; the axial length occupied by the four turbine stages is also very small (approximately 250 mm).

This brief overview of two intermediate sCO_2 turbomachinery prototypes clearly illustrates the disruptive conceptions involved in sCO_2 turbomachinery developments and the imaginative designs developed by engineers.

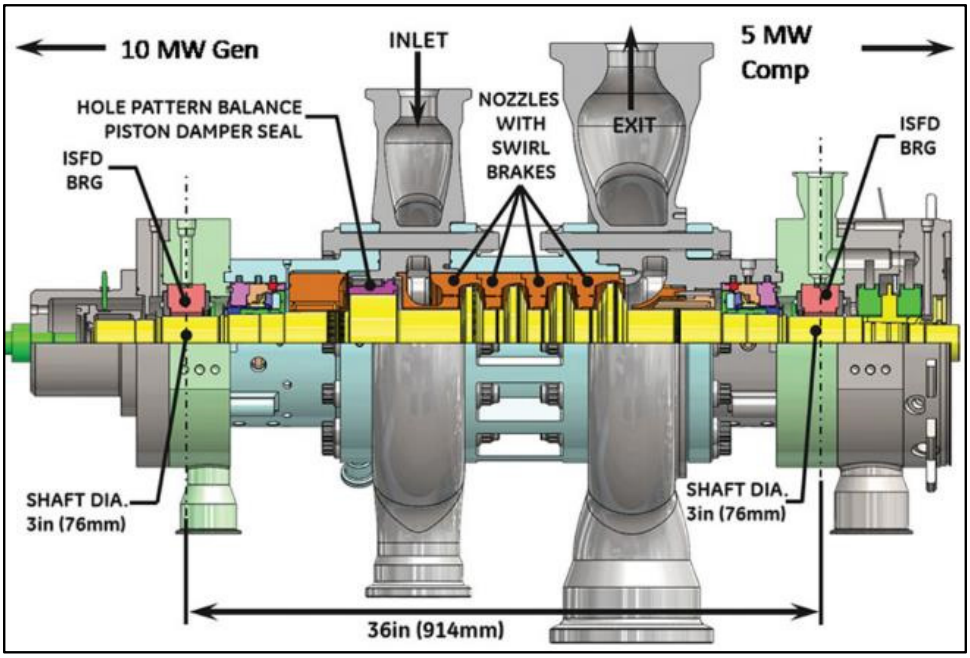

Figure 19. Alternative shaft line arrangement project [56].

7.2. Likely Critical Design Points and Technology Locks

It is now interesting to try to identify and summarize the most important technical challenges underlying these developments.

7.2.1. Metrological Difficulties

First of all, the development of sCO_2 cycles poses a very specific metrological issue due to the fact that, in the vicinity of the saturation curve and more particularly of the critical point, it becomes difficult to carry out, with adequate accuracy, the physical measurements needed during the engineering tests to determine prototype performances [57]. This comes from strong variations in density, Cp and speed of sound in this specific region of the P-T diagram; the speed of sound is important in high-speed flows of turbomachines because it determines local Mach numbers.

7.2.2. Rotor Dynamic Stability of Turbomachines

The mechanical design of turbomachines must take into account, from a dynamic point of view, an important specificity of critical fluids, namely their high densities and little compressibility which impacts on critical speed and vibration levels. Fast load variations are conducive to steep torque variations of the turbine rotor. This both increases radial imbalances on it and generates strong accelerations/decelerations of its rotation due to its small mechanical inertia; this also causes strong axial thrusts [56]. Hydraulic turbines use also a dense fluid (water); however, the inertia of their rotor is much greater and the water flow is cold and virtually isothermal (no thermal stresses). In addition, they operate in open cycle mode, unlike the closed nature of RCBCs in which a change in state of one component (e.g., the turbine) results in retroactions from others, with the possibility of cascading effects and even resonance events.

Changes in regime, whether programmed or unplanned (trips of the unit), must therefore be anticipated during design and carefully analyzed and controlled.

7.2.3. Strong Pressure Gradients and Variations during Transient Regimes

Likewise, it is necessary that all components feature mechanical resistance adapted to the pressure variations (over time) and the gradients (between the P- and P+ cycle branches) which prevail during starts, load variations, stops and trips that may occur

from full load. Indeed, these transient effects, similar to "water hammers", may generate intense and sudden pressure differences between the "P+" and "P-" branches of several components; this is of special concern in heat exchangers which must have therefore adequate material over-thickness.

7.2.4. High Thermal Gradients

In high temperature sCO_2 cycle applications, the expansion process creates by definition important thermal gradients along the turbine rotor [54].

The point is that the short length of the latter means that these gradients concentrate on short axial sections of the shaft. The more localized expansion/contraction processes which result cause important mechanical stresses to the material and significant localized expansions/contractions which require cautious studies in terms of component "lifing" (thermal fatigue effects), with the need to select proper metal alloys.

7.2.5. Control of CO_2 Leaks

Leaks of the working fluid are critical in any closed cycles and even more so when operating for long periods under high pressure, with the requirement of a very strict tightness [58]. Conventional refrigerators and heat pumps operate also in close loop but they are less subject to this issue due to quite moderate pressures.

CO_2 leak rates are magnified by the high operation pressures (up to 250 or even 300 bar) and the high recirculation rates due to the low values of the SPOs.

Yet it is essential to reduce leaks at turbomachine bearings to a strict minimum, for several reasons:

- to control and minimize CO_2 consumption
- to reduce efficiency penalties ("CO_2 that has leaked no longer works in the turbine")
- to minimize health and safety risks (asphyxiation)
- finally, to quickly access the targeted stationary regimes, as CO_2 leaks imply deviations in operating parameters (flow rates; pressures; temperatures).

In comparison, when a steam turbine leaks, the resulting H_2O losses are environmentally benign and do not induce excessive additional costs on the site where this machine is installed, because there are generally adequate water resources on the spots. As far as GTs are concerned, air leaks (essentially at the compressor rear bearing when it exists) and combustion gas leaks (at the rear turbine bearing) are less critical because (i) the pressures are relatively modest (maximum 30 bar) and (ii) since air Brayton cycles are open, the leaks do not impact on the cycle fluid inventory; they are diluted by air venting and evacuated from the enclosure which surrounds the machine.

The case is different for sCO_2 cycles because carbon dioxide is a manufactured product which must be purchased, transported and stored under pressure while complying with strict safety measures.

Figure 20 illustrates the engineering challenge posed by reducing leak rates at a suitable level under the STEP program [58]. While, in current turbine technologies, leaks represent on average 0.4% of the passing flow rates, the objective to be achieved in sCO_2 closed cycles is a maximum leak rate of around 0.02% at turbine bearings.

It is therefore, ultimately, a question of achieving a very high degree of tightness, unprecedented in the history of turbomachines in power generation applications.

To achieve such an ambitious target, researchers have developed innovative sealing devices involving very specific designs, such as that based on the injection of "counter-flows" of CO_2 into turbine labyrinths [59]. We easily realize the complexity added by these devices to solve a problem which had not even been envisaged by the inventors of the sCO_2 power path and the consequences in terms of design: "the devil is in the details! "...

The whole CO_2 storage and circuitry, called the "fluid inventory", has then become an integral system item of the cycle [60].

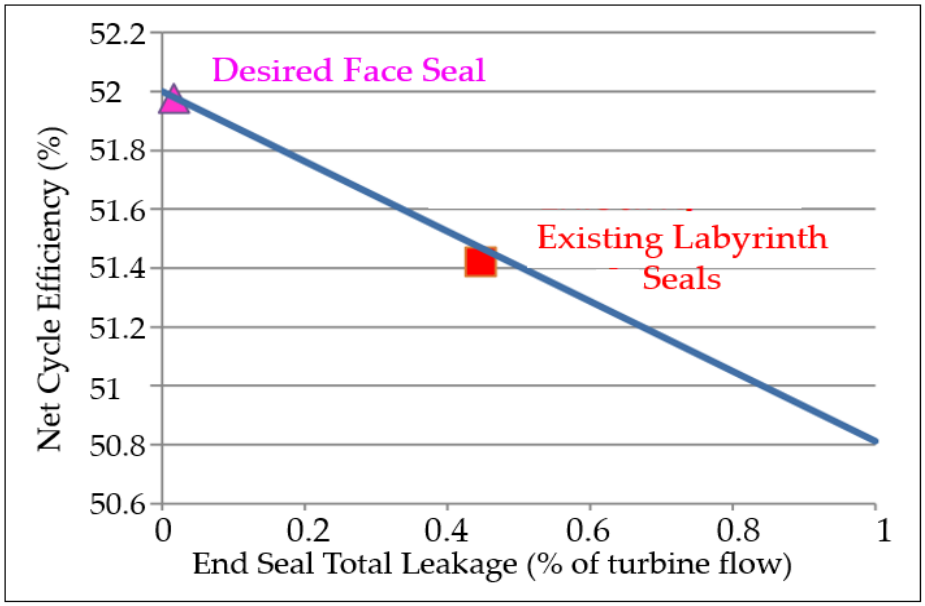

Figure 20. Objective for the leak minimization at sCO_2 turbine bearings [58].

7.2.6. Turbomachinery Efficiency

The levels of isentropic efficiencies mentioned above for turbines et compressors are still modest and must/will be increased as development progresses. The point is that most advanced sCO_2 Brayton cycles (RCBC) include two compressors and at least one turbine and even more in the case of multiple heat recovery, as set out in § 6.2. The overall electrical efficiency gets "eroded" when the number of turbomachines increases.

This is a major task to conduct in order to be able to cope with and exceed the performance of steam cycles not only in "ideal" conditions but also in real ones. This requires long and costly aerodynamic, thermal and mechanical studies [61,62].

8. Conclusions

Supercritical CO_2 cycles offer a rare opportunity for significant efficiency gains in electric power generation, which would greatly benefit the energy transition. However, since its discovery in the late 1960s, the translation of this technology into real large power units seems slow to happen.

In that context, the main motivation of this article was to investigate the possible reasons for this unexpectedly long industrialization process.

Pursuing this goal required a dive into the science of sCO_2 cycles, which led us to address the following aspects of that technology: (i) the classification and architectures of cycles, (ii) their thermodynamics and (iii) their conceptual advantages and drawbacks. To judge their actual merits, we were also led to compare their theoretical energy performances to those of conventional power generation paths.

Fundamentally, the technology has really a significant potential in terms of efficiency enhancement and reduction in component sizes. The efficiency comes from the favorable balance of compressions and expansions which is inherent to supercritical fluids. The advantage of reduced components size is tied to the high "energy density" of supercritical fluids compared to those of steam and air used in conventional Rankine and Brayton cycles, respectively.

The thermodynamic evaluation of the possible architectures carried out in our work confirms that the RCBC (Recompressed Closed Brayton Cycle) architecture is the most promising within the energy transition process, with an ideal efficiency reaching 48% as soon as the heat source attains 550 °C, rivaling thus with most modern gas turbines fired at 1400–1500 °C.

The turbomachine prototypes resulting from the development programs carried out to date confirm the significant gain in component size; this is despite the low specific power outputs (SPO) of the cycles which result from the necessarily low pressure ratios.

In addition, the number of auxiliary components will be considerably reduced compared to steam Rankine units which need a complex set of auxiliaries. In other words, the complexity and footprint of the balance of plant (BOP) will be reduced, which will have favorable impacts on CAPEX and O&M expenditures [63].

The need for intense heat recuperation to compensate for the low specific outputs is no longer an obstacle thanks to the availability of very compact and efficient heat exchangers, notably those of the PCHE technology [64].

However, improving efficiency is probably the "mother of battles" that engineers must win in the next development cycles if we want sCO_2 cycles to be highly efficient and become instrumental in the energy transition. Indeed, the actual energy performances of Brayton sCO_2 cycles strongly depend on the isentropic efficiencies of the set of turbomachines they need for their operation, which comprises at least two compressors and one turbine. These machines have strong operational specificities and their development faces multiple and unprecedented technical challenges, namely (i) to ensure the rotational stability of the composite shaft, (ii) to cope with the strong pressure variations (over time) and gradients (between circuit branches), (iii) to bring the level of leaks at turbine bearings to an unprecedentedly low level despite the high pressures and, especially, (iv) to improve the isentropic efficiencies of the compressors and the turbine.

The validation and improvement of turbomachine technology therefore seems to be the stumbling block for the success of that technology and its deployment in large power generation blocks.

Author Contributions: Conceptualization, M.M.; methodology, R.P., M.M. and J.-N.J.; software, R.P.; validation, J.-N.J. and F.G.; formal analysis, M.M., R.P. and F.G.; investigation, M.M.; resources, M.M.; data curation, R.P. and J.-N.J.; writing—original draft preparation, M.M.; writing—review and editing, J.-N.J. and F.G.; visualization, M.M.; supervision, R.P. and J.-N.J.; project administration, R.P and J.-N.J.; funding acquisition, no funding. All authors have read and agreed to the published version of the manuscript.

Funding: This research received no external funding.

Data Availability Statement: Data supporting reported results can be obtained from authors through an email request addressed to the corresponding author.

Conflicts of Interest: The authors declare no conflict of interest.

Appendix A. Attempts to Increase the Critical Temperature in sCO_2 Rankine Cycles

An approach for increasing the critical temperature in sCO_2 Rankine cycle consists in looking for a substance "X" that, once blended with CO_2, would increase the Tc value by 15 °C, for example.

Such substance X can be a hydrocarbon, a halogenated hydrocarbon or even an inorganic compound like volatile transition metal chlorides. In addition, it must meet a strict EHS specification, for instance:

- GWP (Global Warming Potential): ≤ 1
- ODP (Ozonic Depletion Potential): 0
- Toxicity: not acute
- Fire protection: must not be flammable if in contact with air (case of leaks)
- Chemical stability: must be stable in presence of humidity
- Thermal stability: must at least higher than 350 °C (according to application)
- Cost: must be reasonable for economic viability

However, the search for such X-molecules has proven disappointing. Indeed, the only candidates capable of increasing Tc are chemical species which either do not meet the above specification (being e.g., flammable, unstable or toxic) or present strong structural

differences compared to CO_2, which is a small, symmetric and nonpolar molecule. Indeed, such dissimilarities-in terms of size, polarity or lack of symmetry-result in an inclination of the condensation plateau which causes a decrease of the bubble temperature "T_b", while the dew point "T_{dp}" increases.

This "gliding effect" thus opposes the objective of fully condensing CO_2 at a higher temperature. Figure A1 illustrates the cases of two such molecules noted X′ and X″ (X″ being here bigger than X′).

For example, we tested propane (X′ = C_3H_8) and dimethyl ether (X″ = C_2H_6O) while other researchers had tested X″ = $TiCl_4$ [36] and C_6F_6 [37].

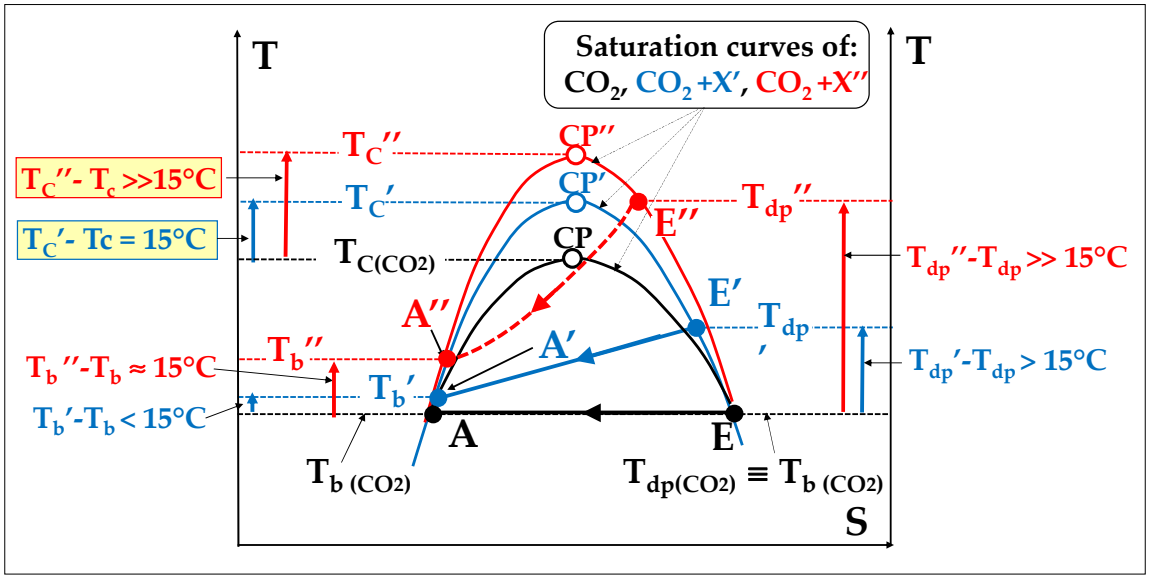

Figure A1. Changes to the isothermal condensation plateau occurring when adding a molecule (X′ or X″) heavier than CO_2; points A, A′, A″ and E, E′, E″ refer to the condensation stage of Figure 1C.

A reasonable addition of X′ (e.g., 20% by mole) allows an increase of Tc by 15 °C but the increase in T_b is unfortunately tiny. In turn, a reasonable addition of X″ allows an increase in Tc of more than 15 °C but the increase in T_b will be barely 15 °C. In addition, a heavy species like X″ causes a more or less marked curvature of the plateau upwards. This effect is undesirable because, if the dew point (E″ mark) goes too close to the critical point (CP), the control process of the cycle becomes delicate due to strong metrological inaccuracies near the critical point [57].

These attempts made by us and others [36,37] then turn to be unsuccessful.

References

1. STEP 10 MWe Pilot (NETL). Available online: https://netl.doe.gov/carbon-management/sco2/step10pilotplant (accessed on 22 January 2024).
2. Marion, J. Supercritical CO_2-10 MW Demonstration project under construction. *Turbomachinery Magazine*, 22 October 2022. Available online: https://www.gti.energy/wp-content/uploads/2022/09/Supercritical-CO2-10-MW-Demonstration-Project-Under-Construction-Sept-Oct-2022.pdf (accessed on 22 January 2024).
3. Allam, R.J.; Palmer, M.R.; Brown, G.W.; Fetvedt, J.; Freed, D.; Nomoto, H.; Itoh, M. High efficiency and low cost of electricity generation from fossil fuels while eliminating atmospheric emissions 2013. *Energy Procedia* **2013**, *37*, 1135–1149. [CrossRef]
4. Angelino, G. Perspectives for the Liquid Phase Compression Gas Turbine. *J. Eng. Power* **1967**, *89*, 229–236. [CrossRef]
5. Angelino, G. Carbon dioxide condensation cycles for power production. *J. Eng. Power* **1968**, *90*, 287–295. [CrossRef]
6. Angelino, G. Real gas effects in carbon dioxide cycles. In Proceedings of the ASME 1969 Gas Turbine Conference and Products Show, Cleveland, OH, USA, 9–13 March 1969. paper No 69GT.103.
7. Feher, E.G. The supercritical thermodynamic power cycle. *Energy Convers* **1968**, *8*, 85–90. [CrossRef]
8. Hoffmann, J.R.; Feher, E.G. 150 kWe Supercritical Closed Cycle System. *J. Eng. Power* **1971**, *93*, 70–80. [CrossRef]
9. Gokhshtein, D.P.; Verkhivker, G.P. Use of Carbon Dioxide as a Heat Carrier and Working Substance in Atomic Power Stations. *Sov. At. Energy* **1969**, *26*, 430–432. [CrossRef]

10. Brown, D.H.; Corman, J.C.; Fleming, R.B. Energy Conversion Alternatives Study (ECAS), General Electric Phase I. Final Report. Volume II. Advanced Energy Conversion Systems. Part 2. Closed Turbine Cycles. Available online: https://www.osti.gov/biblio/7219165 (accessed on 22 January 2024).
11. Moore, J.; Cich, D.; Day, M.; Allison, T.; Wade, J.; Hofer, D. Commissioning of a 1 MWe supercritical CO_2 test loop. In Proceedings of the 6th International Supercritical CO_2 Power Cycles Symposium, Pittsburgh, PA, USA, 27–29 March 2018.
12. Conboy, T.M.; Pasch, J.; Fleming, D. Control of a supercritical CO_2 recompression Brayton cycle demonstration loop. In Proceedings of the ASME Turbo Expo 2013 Turbine Technical Conference and Exposition, San Antonio, TX, USA, 3–7 June 2013.
13. Wright, S.A.; Radel, R.F.; Vernon, M.E.; Rochau, G.E.; Pickard, P.S. Sandia Report: Operation and Analysis of a Supercritical CO_2 Brayton Cycle. 2010. Available online: https://www.osti.gov/servlets/purl/984129 (accessed on 21 January 2024).
14. Clementoni, E.M.; Cox, T.L.; Sprague, C.P. Startup and operation of a supercritical carbon dioxide Brayton cycle. *J. Eng. Gas. Turbines Power* **2014**, *136*, 071701. [CrossRef]
15. Utamura, M.; Hasuike, H.; Ogawa, K.; Yamamoto, T.; Fukushima, T.; Watanabe, T.; Himeno, T. Demonstration of supercritical CO_2 closed regenerative Brayton cycle in a bench scale experiment. In Proceedings of the ASME Turbo Expo, Copenhagen, Denmark, 11–15 June 2012.
16. Cho, J.; Shin, H.; Cho, J.; Kang, Y.S.; Ra, H.S.; Roh, C.; Lee, B.; Baik, Y.J. Preliminary power generating operation of the supercritical carbon dioxide power cycle experimental test loop. In Proceedings of the 6th International Supercritical CO_2 Power Cycles Symposium, Pittsburgh, PA, USA, 27–29 March 2018.
17. Ahn, Y.; Bae, S.J.; Kim, M.; Cho, S.K.; Baik, S.; Lee, J.I.; Cha, J.E. Review of supercritical CO_2 power cycle technology and current status of research and development. *Nucl. Eng. Technol.* **2015**, *47*, 647–661. [CrossRef]
18. Park, J.H.; Bae, S.W.; Park, H.S.; Cha, J.E.; Kim, M.H. Transient analysis and validation with experimental data of supercritical CO_2 integral experiment loop by using MARS. *Energy* **2018**, *147*, 1030–1043. [CrossRef]
19. National Energy Technology Laboratories-Sunshot-Concentrated Solar Power. Available online: https://www.nrel.gov/docs/fy12osti/55455.pdf (accessed on 22 January 2024).
20. United States Department of Energy (US DOE). Sunshot Program. Available online: https://www.energy.gov/sites/prod/files/2019/11/f68/DOE%20sCO2%20Workshop,%20SWRI,%20Jeff%20Moore.pdf (accessed on 22 January 2024).
21. USDOE-DOE. Announces $80 Million Investment to Build Supercritical Carbon Dioxide Pilot Plant Test Facility. Available online: https://www.energy.gov/articles/doe-announces-80-million-investment-build-supercritical-carbon-dioxide-pilot-plant-test (accessed on 22 January 2024).
22. National Energy Technology Laboratory. STEP 10 MWe. Supercritical Transformational Electric Power. Available online: https://netl.doe.gov/carbon-management/sco2/step10pilotplant (accessed on 22 January 2024).
23. A Step Forward for sCO_2 Power Cycles. Modern Power Systems, 9 January 2024. Available online: https://www.modernpowersystems.com/features/featurea-step-forward-for-sco2-power-cycles-11423286/ (accessed on 22 January 2024).
24. Guo, J.Q.; Li, M.J.; He, Y.L.; Jiang, T.; Ma, T.; Xu, J.L.; Cao, F. A systematic review of supercritical carbon dioxide (S-CO_2) power cycle for energy industries. *Energy Convers. Manag.* **2022**, *258*, 115437. [CrossRef]
25. Zhao, Q.; Mecheri, M.; Neveux, T.; Privat, R.; Jaubert, J.N. On the selection of a proper equation of state for the modeling of a supercritical CO_2 Brayton cycle: Consequences on the process design. *Ind. Eng. Chem. Res.* **2017**, *56*, 6841–6853. [CrossRef]
26. Dostal, V.; Driscoll, M.J.; Hejzlar, P.; Todreas, N.E. A Supercritical CO_2 Gas Turbine Power Cycle for Next-Generation Nuclear Reactors. In Proceedings of the 10th International Conference on Nuclear Engineering, Arlington, VA, USA, 14–18 April 2002.
27. Rochau, G.E.; Pasch, J.J.; Carlson, M.D.; Fleming, D.D.; Kruizenga, A.M.; Sharpe, R.A.; Wilson, M.C. Supercritical CO_2 Brayton Cycles. Available online: https://www.osti.gov/biblio/1221819 (accessed on 22 January 2024).
28. Weiland, N.T.; Dennis, R.A.; Ames, R.; Lawson, S.; Strakey, P. Fossil Energy. In *Fundamentals and Applications of sCO_2 Based Power Cycles*; Woodhead Publishing: Cambridge, MA, USA, 2017; p. 298.
29. Marion, J. Supercritical CO_2 10 MW Demonstration Project Under Construction. Turbomachinery International, September–October 2022. Available online: https://www.gti.energy/wp-content/uploads/2022/09/Supercritical-CO2-10-MW-Demonstration-Project-Under-Construction-Sept-Oct-2022.pdf (accessed on 22 January 2024).
30. Persichilli, M.; Kacludis, A.; Zdankiewicz, E.; Held, T. Supercritical CO_2 Power Cycle Developments and Commercialization: Why sCO_2 Can Displace Steam. In Proceedings of the Power-Gen India & Central Asia 2012, New Delhi, India, 19–21 April 2012.
31. Allison, T.C.; Moore, J.J.; Wilkes, J.C.; Brun, K. Turbomachinery Overview for sCO_2 cycles. In Proceedings of the 46th Turbomachinery & 33th Pump Symposia, Houston, TX, USA, 11–14 September 2017.
32. Hydrocarbon GWPs and Indirect GWPs. Available online: https://www.fluorocarbons.org/environment/climate-change/hydrocarbon-gwps-and-indirect-gwps/ (accessed on 22 January 2024).
33. Nielson, J.; Simpkins, D.; Katcher, K. Techno-Economic Analysis of a Geothermal sCO_2 Thermosiphon Power Plant. In Proceeding of the 7th International Supercritical CO_2 Power Cycles Symposium, San Antonio, TX, USA, 21–24 February 2022.
34. González-Portillo, L.F.; Muñoz-Antón, J.; Martínez-Val, J.M. Supercritical carbon dioxide cycles with multi-heating in Concentrating Solar Power plants. *Solar Energy* **2020**, *207*, 144–156. [CrossRef]
35. US DOE. sCO_2 Power Cycles for Nuclear. Available online: https://www.energy.gov/sco2-power-cycles-nuclear (accessed on 22 January 2024).
36. Bonalumi, D.; Lasala, S.; Macchi, E. CO_2-TiCl4 working fluid for high-temperature heat source power cycles and solar application. *Renew. Energy* **2020**, *147*, 2842–2854. [CrossRef]

37. Crespi, F.; Rodríguez de Arriba, P.; Sánchez, D.; Ayub, B.; Di Marcoberardino, G.; Invernizzi, C.M.; Martínez, G.S.; Iora, P.; Di Bono, D.; Binotti, M.; et al. Thermal efficiency gains enabled by using CO_2 mixtures in supercritical power cycles. *Energy* **2022**, *238*, 121899. [CrossRef]
38. Rogalev, A.; Kindra, V.; Osipov, S.; Rogalev, N. Thermodynamic analysis of the Net Power oxy-combustion cycle. In Proceedings of the 13th European Conference on Turbomachinery Fluid dynamics & Thermodynamics, Lausanne, Switzerland, 8–12 April 2018.
39. Held, T.J. Supercritical CO_2 cycles for Gas turbine Combined Cycle Power Plants. In Proceedings of the Power Gen International, Las Vegas, NV, USA, 8–10 December 2015.
40. Weiland, N.T.; Lance, B.W.; Pidaparti, S.R. sCO_2 Power Cycle Component Cost Correlations from DOE Data Spanning Multiple Scales and Applications. In Proceedings of the ASME Turbo Expo 2019: Turbomachinery Technical Conference and Exposition, Phoenix, AZ, USA, 17–21 June 2019.
41. US DOE. Break-Even Power Transients for Two Simple Recuperated S-CO_2 Brayton Cycle Test Configurations. Available online: https://www.osti.gov/biblio/1108096 (accessed on 22 January 2024).
42. Liese, E.A.; Mahapatra, P.; Albright, J.T.; Zitney, S.E. Regulatory Control of a 10 MWe sCO_2 Recompression Closed Brayton Cycle. Available online: https://www.netl.doe.gov/sites/default/files/2019-05/2019_Annual_Reports/Thursday/Sensors/4%20Liese_NETL_Crosscutting2019_.pdf (accessed on 22 January 2024).
43. Vijaykumar, R. Power Cycles: Supercritical CO_2 Brayton Cycle Development Overview. Available online: https://www.energy.gov/sites/default/files/2020/04/f73/Breakout%20CSP%20Day2%20PowerCycles_Vijaykumar.pdf (accessed on 22 January 2024).
44. Moroz, L.; Frolov, B.; Burlaka, M.; Guriev, O. Turbomachinery Flowpath design ad performance analysis for sCO_2. In Proceedings of the ASME Turbo Expo 2014, Dusseldorf, Germany, 16–20 June 2014.
45. Binotti, M.; Astolfi, M.; Campanari, S.; Manzolini, G.; Silva, P. Preliminary assessment of sCO_2 power cycles for application to CSP Solar Tower plants. *Energy Procedia* **2017**, *105*, 1116–1122. [CrossRef]
46. Vinoya, C.L.; Ubando, A.T.; Culaba, A.B.; Chen, W.H. State-of-the-Art Review of Small Modular Reactors. *Energies* **2023**, *16*(7), 3224. [CrossRef]
47. Zhao, Q.; Mecheri, M.; Neveux, T.; Privat, R.; Jaubert, J.N.; Le Moullec, Y. Search for the optimal design of a supercritical-CO_2 Brayton power cycle from a superstructure-based approach implemented in a commercial simulation software. *Energies* **2023**, *16*, 5470. [CrossRef]
48. Mehos, M.; Turchi, C.; Vidal, J.; Wagner, M.; Ma, Z.; Ho, C.; Ho, C.; Kolb, W.; Andraka, C.; Kruizenga, A. Concentrating Solar Power Gen3 Demonstration Roadmap. Technical Report. Available online: https://www.nrel.gov/docs/fy17osti/67464.pdf (accessed on 22 January 2024).
49. Quaschning, V.; Geuder, N.; Richter, C.; Trieb, F. Contribution of CSP for Competitive Sustainable Energy Supply. Available online: https://www.volker-quaschning.de/downloads/CleanAir2003.pdf (accessed on 22 January 2024).
50. Bonalumi, D.; Giuffrida, A.; Sicali, F. Thermo-economic analysis of a supercritical CO_2-based waste heat recovery system. In Proceedings of the 76th Italian Conference ATI, Roma, Italy, 15–17 September 2021.
51. Yuri, M.; Masada, J.; Tsukagoshi, K.; Ito, E.; Hada, S. Development of 1600 °C-Class High-Efficiency Gas turbine for Power Generation Applying J-Type Technology. *MHI Tech. Rev.* **2013**, *40*, 1–10.
52. US DOE-Advanced Gas Turbine and sCO_2 Combined Cycle Power System. Available online: https://www.netl.doe.gov/sites/default/files/2019-01/FE0031619-kickoff.pdf (accessed on 22 January 2024).
53. Can Gulen, S. Study on Gas Turbine Combined Cycle Power Plant—Next 20 Years. *J. Eng. Gas Turbines Power* **2016**, *138*, 051701. [CrossRef]
54. Bidkar, A.R.; Mann, A.; Singh, R.; Sevincer, E.; Cich, S.; Day, M.; Kulhanek, C.D.; Thatte, A.M.; Peter, A.M.; Hofer, D.; et al. Conceptual Designs of 50 MWe and 450 MWe Supercritical CO_2 Turbomachinery Trains for Power Generation from Coal. Part 1: Cycle and Turbine. In Proceedings of the 5th International Symposium-Supercritical CO_2 Power Cycles, San Antonio, TX, USA, 28–31 March 2016.
55. Bidkar, A.R.; Musgrove, G.; Day, M.; Kulhanek, C.D.; Allison, T.; Peter, A.M.; Hofer, D.; Moore, J.J. Conceptual Designs of 50 MWe and 450 MWe Supercritical CO_2 Turbomachinery Trains for Power Generation from Coal, Part 2: Compressors. In Proceedings of the 5th International Symposium-Supercritical CO_2 Power Cycles, San Antonio, TX, USA, 28–31 March 2016.
56. Moore, J.J. Status of sCO_2 Turbomachinery Development at SwRI. Available online: https://sco2symposium.com/proceedings2022/jeff-moore-panel1.pdf (accessed on 22 January 2024).
57. Mortzheim, J.; Hofer, D.; Priebe, S.; McClung, A.; Moore, J.J.; Cich, S. Challenges with Measuring Supercritical CO_2 Compressor Performance When Approaching the Liquid-Vapor Dome. In Proceedings of the ASME Turbo Expo 2021—Turbomachinery Technical Conference and Exposition, Virtual, 7–11 June 2021. Available online: https://asmedigitalcollection.asme.org/GT/proceedings-abstract/GT2021/85048/V010T30A019/1120350?redirectedFrom=PDF (accessed on 22 January 2024).
58. Bidkar, R.; Allison, T.; Hofer, D.; Brun, K.; Kalra, C.; Cich, S.; Mann, A.; Day, M.; Peter, M.; Kulhanek, C.; et al. sCO_2 turbomachinery and ow-leakage sCO_2 end seals. Available online: https://netl.doe.gov/sites/default/files/event-proceedings/2015/utsr/GE_sCO2seals_UTSR_website_version.pdf (accessed on 22 January 2024).
59. Stahley, J. Dry Gas Seal System Design Standards for Centrifugal Compressor Applications. In Proceedings of the 31st Turbomachinery Symposium, College Station, TX, USA, 21–24 April 2002.

60. Tom, B.; Smith, J.; Day Towler, M. Inventory Management Operational Strategies for a 10 MWe sCO_2 Power Block. In Proceedings of the 7th International sCO_2 Power Cycles Symposium, San Antonio, TX, USA, 21–24 February 2022.
61. Kim, T.W.; Kim, N.H.; Suh, K.Y. Computational Analysis of sCO_2 Flow Around a Turbine and Compressor Blade. In Proceedings of the 15th International Conference on Nuclear Engineering, Nagoya, Japan, 22–26 April 2007.
62. Li, Z.; Bian, W.; Jiang, L.; Liu, C.; Shi, J.; Hao, N. sCO_2 Turbine Design and Arrangement Optimization. *Front. Energy Res.* **2022**, *10*, 922542. [CrossRef]
63. USDOE. sCO_2 Power Cycle Component Cost Correlations from DOE Data Spanning Multiple Scales and Applications. Available online: https://www.osti.gov/servlets/purl/1601743 (accessed on 22 January 2024).
64. Bahmann, Z. Heat Exchanger Types and Classifications. In *Compact Heat Exchangers*, 2nd ed.; Elsevier: New York, NY, USA, 2016; Chapter 2.